

AD-778 430

PARAMETRIC STUDY OF HYPERSONIC TUR-
BULENT BOUNDARY LAYERS WITH HEAT
TRANSFER

J. S. Shang

Aerospace Research Laboratories
Wright-Patterson Air Force Base, Ohio

January 1974

DISTRIBUTED BY:

NTIS

National Technical Information Service
U. S. DEPARTMENT OF COMMERCE
5285 Port Royal Road, Springfield Va. 22151

NOTICES

When Government drawings, specifications, or other data are used for any purpose other than in connection with a definitely related Government procurement operation, the United States Government thereby incurs no responsibility nor any obligation whatsoever; and the fact that the Government may have formulated, furnished, or in any way supplied the said drawings, specifications, or other data, is not to be regarded by implication or otherwise as in any manner licensing the holder or any other person or corporation, or conveying any rights or permission to manufacture, use, or sell any patented invention that may in any way be related thereto.

Organizations or individuals receiving reports via Aerospace Research Laboratories automatic mailing lists should refer to the ARL number of the report received when corresponding about change of address or cancellation. Such changes should be directed to the specific laboratory originating the report. Do not return this copy; retain or destroy.

Reports are not stocked by the Aerospace Research Laboratories. Copies may be obtained from:

National Technical Information Services
Clearinghouse
Springfield, VA 22151

This technical report has been reviewed and is approved for publication.

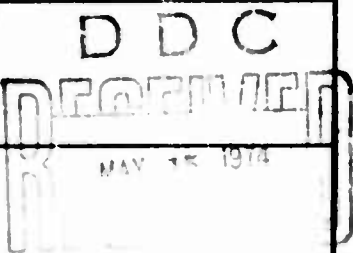
| | | |
|-------------------------------------|---------------|-------------------------------------|
| NTIS | Write Section | <input checked="" type="checkbox"/> |
| DC | Data Section | <input type="checkbox"/> |
| ORNL | | <input type="checkbox"/> |
| DISSEMINATION | | |
| BY _____ | | |
| LIC. RESTRICTION/AVAILABILITY CODES | | |
| Dist. & Avail. Report Special | | |
| A | | |

This report has been reviewed and cleared for open publication and public release by the appropriate Office of Information in accordance with AFR 190-12 and DODD 5230.0. There is no objection to unlimited distribution of this report to the public at large, or by DDC to the National Technical Information Service.

AD-778430

UNCLASSIFIED

SECURITY CLASSIFICATION OF THIS PAGE (When Data Entered)

| REPORT DOCUMENTATION PAGE | | READ INSTRUCTIONS BEFORE COMPLETING FORM |
|--------------------------------------------------------------------------------------------------------------------------------------------------------------------------------------------------------------------------------------------------------------------------------------------------------------------------------------------------------------------------------------------------------------------------------------------------------------------------------------------------------------------------------------------------------------------------------------------------------------------------------------------------------|------------------------------------------------------------|---------------------------------------------------------------------------------------|
| 1. REPORT NUMBER ARL 74-0003 | 2. GOVT ACCESSION NO. | 3. RECIPIENT'S CATALOG NUMBER |
| 4. TITLE (and Subtitle) A PARAMETRIC STUDY OF HYPERSONIC TURBULENT BOUNDARY LAYERS WITH HEAT TRANSFER | | 5. TYPE OF REPORT & PERIOD COVERED TECH REPORT - Interim |
| | | 6. PERFORMING ORG. REPORT NUMBER |
| 7. AUTHOR(s) J. S. SHANG | | 8. CONTRACT OR GRANT NUMBER(s) |
| 9. PERFORMING ORGANIZATION NAME AND ADDRESS Aerospace Research Laboratories (AFSC) Hypersonic Research Laboratory (LH) Wright-Patterson AFB, OH 45433 | | 10. PROGRAM ELEMENT, PROJECT, TASK AREA & WORK UNIT NUMBERS 61102F; 7064-03-07 |
| 11. CONTROLLING OFFICE NAME AND ADDRESS Aerospace Research Laboratories (AFSC) Hypersonic Research Laboratory (LH) Wright-Patterson AFB, OH 45433 | | 12. REPORT DATE January 1974 |
| | | 13. NUMBER OF PAGES 48 |
| 14. MONITORING AGENCY NAME & ADDRESS (if different from Controlling Office) | | 15. SECURITY CLASS. (of this report) Unclassified |
| | | 15a. DECLASSIFICATION/DOWNGRADING SCHEDULE |
| 16. DISTRIBUTION STATEMENT (of this Report) Approved for public release; distribution unlimited. | | |
| 17. DISTRIBUTION STATEMENT (of the abstract entered in Block 20, if different from Report) | | |
| 18. SUPPLEMENTARY NOTES | | |
| 19. KEY WORDS (Continue on reverse side if necessary and identify by block number) | | |
| Fluctuating Density | Numerical solutions |  |
| Turbulent boundary layer | Reproduced by NATIONAL TECHNICAL INFORMATION SERVICE | |
| Shear Stress | U S Department of Commerce Springfield VA 22151 | |
| | | |
| 20. ABSTRACT (Continue on reverse side if necessary and identify by block number) | | |
| <p>Models of the Reynolds shear stress and the turbulent energy flux are modified to include the effect of fluctuating density for the hypersonic flow regime. The compressible turbulent boundary layer equations are solved by a finite difference scheme. The results, when compared with experimental measurements at hypersonic flow conditions, indicate a meaningful improvement in predicting the skin friction coefficient. Excellent comparison between the data and the calculations is also attained in the laminar and transition region. The static pressure variation across a turbulent boundary layer is also investigated in the</p> | | |

DD FORM 1473 1 JAN 73 EDITION OF 1 NOV 65 IS OBSOLETE

UNCLASSIFIED

SECURITY CLASSIFICATION OF THIS PAGE (When Data Entered)

20. (Cont'd)

present analysis by including the normal momentum equation. The normal momentum equations reveals that the sum of static pressure and the normal component of the Reynolds shear stress is an invariant across a turbulent boundary layer. A tentative model for the fluctuating velocity term is proposed and the resulting pressure variation across the boundary layer confirmed by experimental measurements. The sensitivity of a turbulent Prandtl number variation throughout the turbulent boundary layer is also evaluated. Numerical solutions exhibited a weak dependence on the turbulent Prandtl number variations.

PREFACE

The report was prepared by the Hypersonic Research Laboratory of the Aerospace Research Laboratories, Air Force Systems Command, United States Air Force, under Project 7064, entitled "High Velocity Fluid Mechanics," project monitor Dr. R. H. Korkegi. This is an interim report.

TABLE OF CONTENTS

| SECTION | | PAGE |
|---------|-----------------------------------|------|
| I | INTRODUCTION. | 1 |
| II | GOVERNING EQUATIONS | 3 |
| III | EDDY VISCOSITY MODEL. | 7 |
| IV | TURBULENT PRANDTL NUMBER. | 11 |
| V | DISCUSSION OF RESULTS | 12 |
| VI | CONCLUDING REMARKS. | 21 |
| | REFERENCES. | 37 |

LIST OF ILLUSTRATIONS

| FIGURE | | PAGE |
|--------|--------------------------------------------------------------------------------------------------------------|------|
| 1 | Correlations of the turbulent kinetic energy, the Reynolds shear stress and $\langle v'^2 \rangle$ | 23 |
| 2 | The uncertainty envelope of the turbulent Prandtl number and the approximated Pr_t distributions. | 24 |
| 3 | Static pressure distribution across turbulent boundary layer. . | 25 |
| 4 | Effect of variable turbulent Prandtl number on C_f and St | 26 |
| 5 | Effect of variable turbulent Prandtl number on temperature profile | 27 |
| 6 | Effect of constant turbulent Prandtl number on temperature and velocity profiles | 28 |
| 7 | Effect of constant turbulent Prandtl number on the eddy viscosity coefficient distribution. | 29 |
| 8 | Nondimensional total enthalpy versus velocity | 30 |
| 9 | Effect of density fluctuation on C_f and St at $M_e = 7.4$ | 31 |
| 10 | Effect of density fluctuation on C_f and St at $M_e = 8.0$ | 32 |
| 11 | Effect of density fluctuation on C_f and St at $M_e = 10.5$ | 33 |
| 12 | Effect of density fluctuation on C_f and St at $M_e = 12$ | 34 |
| 13 | Skin friction coefficient variation with Mach number. | 35 |
| 14 | Effect of damping constant on C_f | 36 |

LIST OF SYMBOLS

| | |
|------------------|--------------------------------------------------------------------------------------------------------------------------------------------------------------------------------------------------------|
| C_f | Skin friction coefficient |
| C_p | Specific heat at constant pressure |
| C | Viscosity-density parameter |
| F | Dimensionless velocity u/u_e |
| h | Static enthalpy |
| H | Total enthalpy |
| k_1, k_2 | Constants in eddy viscosity models |
| M | Mach number |
| P | Pressure |
| Pr | Molecular Prandtl number $\mu C_p / \lambda = 0.73$ |
| Pr_1, Pr_2 | Constants in Eq. (25) |
| Pr_t | Turbulent Prandtl number $Pr_t = \rho C_p \epsilon / \lambda t = \langle u'v' \rangle \left(\frac{\partial T}{\partial y} \right) / \left(\langle vT' \rangle \frac{\partial u}{\partial y} \right)$ |
| Q | Rate of heat transfer at the wall |
| St | Stanton number - $Q / \rho_e u_e (H_0 - h_w)$ |
| T | Static temperature |
| u, v | Streamwise and normal velocity components |
| α | $u_e^2 / C_p T_e$ |
| α_{xyz} | Correlation constant |
| β | $2\xi / u_e (du_e / d\xi)$ |
| γ | Ratio of specific heats |
| ϵ | Kinematic eddy viscosity coefficient |
| $\bar{\epsilon}$ | Dimensionless equivalent viscosity $1 + \epsilon \Gamma / \nu$ |
| $\hat{\epsilon}$ | Dimensionless equivalent viscosity $1 + (Pr / Pr_t)(\epsilon \Gamma / \nu)$ |
| θ | Dimensionless temperature T / T_e |
| θ | Boundary layer momentum thickness |

| | |
|----------------------|-------------------------------------------------------|
| λ, λ_t | Molecular and apparent turbulent thermal conductivity |
| μ | Molecular viscosity coefficient |
| ν | Molecular kinematic viscosity |
| ξ, η | Transformed streamwise and normal coordinates |
| ρ | Density |
| τ | Shear stress |

Subscripts

| | |
|------------------|-----------------------------------------------------|
| e | Denotes variable evaluated at local external stream |
| t,i | Beginning of transition |
| t,f | End of transition |
| w | Denoted variable evaluated at wall |
| < > | Time-mean average |

SECTION I

INTRODUCTION

The concept of eddy viscosity has been applied to predict turbulent boundary layers in hypersonic flow regions.^(1,2,3) Hopkins et al. found that the multilayer eddy viscosity model by Cebeci⁽⁴⁾ underpredicted the skin friction coefficient by around 10% for hypersonic flow conditions. Extension of the essentially incompressible eddy viscosity model to compressible flow is based on the fact that the turbulence producing mechanism remains similar in spite of the presence of temperature or density fluctuations. The prediction of compressible turbulent boundary layers by eddy viscosity models indeed yields essential agreement with experimental data up to a Mach number of five.^(1,4,5) However, in the hypersonic flow region Bushnell and Beckwith revealed a dependence of the Reynolds stress on the density fluctuations. In fact, Bushnell⁽¹⁾ introduced a mixing length model for the density fluctuations in his formulation of the apparent viscosity coefficient. A few specific comparisons were made to illustrate the effect of the fluctuating property on the mean flow.

Recent experimental data recorded^(6,7,8) at high Mach numbers reveals significant pressure fluctuations in the turbulent boundary layer. A common characteristic of the measured pressure data^(6,7) indicates a distinct normal pressure gradient within the turbulent boundary layer. At the present time, no analytical method has been developed to include this phenomena.

Numerical solutions of the compressible turbulent boundary layer with heat transfer are commonly obtained by assuming a constant turbulent Prandtl number. The Prandtl number is generally assigned to be near unity. Recently, extensive experiments have been devoted to studying

the Prandtl number distribution across the turbulent boundary layer. The work on the turbulent Prandtl number by Meier and Rotta⁽⁹⁾ revealed that the turbulent transport of energy decreases more rapidly toward the wall than the momentum transport. Therefore, the turbulent Prandtl number exceeds the value of unity near the wall but decreases slightly within the sublayer region. Their findings fall within the uncertainty which envelopes the turbulent Prandtl number distribution by Simpson et al.⁽¹⁰⁾ Their results seem to indicate that the heat transfer and temperature profile of turbulent flows cannot be ascertained by an oversimplified constant turbulent Prandtl number. Again, no systematic evaluation of the effect of variable Prandtl number on the heat transfer and temperature distributions in a boundary layer has been performed.

The present analysis intends to investigate the hypersonic turbulent boundary layer with heat transfer. The explicit dependence of the density fluctuation is introduced into the eddy viscosity model in a similar manner to that of Bushnell et al., except that the density fluctuation is derived from the data of Kistler⁽¹¹⁾ instead of by a mixing length concept. The normal pressure gradient in the boundary layer due to turbulence is taken into account by including the y momentum equation of mean motion. The fluctuation term $\langle(\rho v)'v'\rangle$ in the y momentum equation is correlated with the Reynolds shear stress to predict the pressure variation within the boundary layer. The sensitivity of the temperature distribution and heat transfer due to the influence of a turbulent Prandtl number profile variation is examined. Predictions of the velocity, static temperature profiles, as well as the wall skin friction and heat transfer values, are compared with experimental data.

SECTION II
GOVERNING EQUATIONS

The basic equations are written in essentially the form as given by Van Driest⁽¹²⁾ except for the additional normal momentum equation

Continuity

$$\frac{\partial \rho u}{\partial x} + \frac{\partial}{\partial y} [\rho v + \langle (\rho v)' \rangle] = 0 \quad (1)$$

Streamwise momentum equation

$$\rho u \frac{\partial u}{\partial x} + [\rho v + \langle (\rho v)' \rangle] \frac{\partial u}{\partial y} = - \frac{\partial p}{\partial x} + \frac{\partial}{\partial y} \left(\mu \frac{\partial u}{\partial y} \right) - \frac{\partial}{\partial y} [\langle (\rho v)' u' \rangle] \quad (2)$$

Normal momentum equation

$$\frac{\partial}{\partial y} [\langle (\rho v)' v' \rangle + p] = 0 \quad (3)$$

Energy equation

$$\begin{aligned} \rho u \frac{\partial h}{\partial x} + [\rho v + \langle (\rho v)' \rangle] \frac{\partial h}{\partial y} &= \frac{\partial}{\partial y} \left[\frac{k}{C_p} \frac{\partial h}{\partial y} - \langle (\rho v)' h' \rangle \right] \\ + u \frac{dp}{dx} + \left[\mu \frac{\partial u}{\partial y} - \langle (\rho v)' u' \rangle \right] \frac{\partial u}{\partial y} & \end{aligned} \quad (4)$$

To perform calculations of turbulent boundary layers, initial conditions are required together with the usual nonslip condition and matching temperature condition at the wall. The boundary conditions at the outer edge of the boundary layer have u and h approaching u_e and h_e , respectively.

The fluctuation terms can be expanded as follows:⁽¹²⁾

$$\langle (\rho v)' u' \rangle = \rho \langle u' v' \rangle + v \langle \rho' u' \rangle + \langle \rho' u' v' \rangle \quad (5)$$

$$\langle (\rho v)' v' \rangle = \rho \langle v' v' \rangle + v \langle \rho' v' \rangle + \langle \rho' v' v' \rangle \quad (6)$$

$$\langle (\rho v)' h' \rangle = \rho \langle v' h' \rangle + v \langle \rho' h' \rangle + \langle \rho' v' h' \rangle \quad (7)$$

The above turbulent correlation terms are not known a priori. If the above equations are normalized with respect to a reference condition, an estimation

of the aforementioned terms can be made. For a boundary layer this may be done with a standard order of magnitude analysis. Herring and Mellor⁽¹³⁾ have shown the order of magnitude for these turbulent correlations. In their analysis, $\Delta\rho$ and Δh denote the variation of mean density and mean static enthalpy, respectively, across the boundary layer. $\Delta\rho/\rho_e$ is restricted to the order of magnitude of unity. The second term contains v in Eqs. (5), (6) and (7), and v/u_e is proportional to δ/L . Therefore, $v\langle\rho'u'\rangle/u_e^2\Delta\rho$ has the order of $(\delta/L)^2$, where δ is the boundary layer thickness and L is the length of the plate. These terms are neglected by Van Driest⁽¹²⁾ for a thin boundary layer. The order of magnitude of the triple correlation terms in Eqs. (5), (6) and (7) is difficult to assess. For the present purpose, an estimate by their root-mean-square values seems to be adequate. We have $\langle\rho'u'v'\rangle/\rho_e^2 \sim O(\sqrt{\rho'^2}\delta/\rho L)$. A similar argument leads to the identical results for Eqs. (6) and (7). The upper limit of $\sqrt{\rho'^2}/\rho$ can be obtained from the data of Kistler ($\rho'/\rho = -T'/T$). The relative density fluctuation is around one tenth of $2(T_0 - T_\infty)/(T_0 + T_\infty)$ for Mach numbers up to around five. In this form the relative density fluctuation is nearly independent of Mach number. In view of the order of magnitude analysis, the only triple correlations retained in the present analysis are $\langle\rho'u'v'\rangle$, $\langle\rho'v'v'\rangle$ and $\langle\rho'v'h'\rangle$. Viscosity fluctuation is neglected following the work of Bushnell et al.⁽¹⁾

The Reynolds shear stress becomes

$$\langle(\rho v)'u'\rangle = \rho\langle u'v'\rangle \left(1 + \alpha_{\rho uv} \frac{\sqrt{\rho'^2}}{\rho} \right) \quad (8)$$

Similar results can be expressed for Eqs. (6) and (7)

$$\langle(\rho v)'v'\rangle = \rho\langle v'v'\rangle \left(1 + \alpha_{\rho vv} \frac{\sqrt{\rho'^2}}{\rho} \right) \quad (9)$$

$$\langle(\rho v)'h'\rangle = \rho\langle v'h'\rangle \left(1 + \alpha_{\rho vh} \frac{\sqrt{\rho'^2}}{\rho} \right) \quad (10)$$

where the α 's are the correlation functions. The subscripts denote the respective variables to be correlated. Since the density fluctuation is introduced by phenomenological means with uncertainty in the RMS value, the correlation coefficients are assumed to be unity. This assumption has been applied implicitly in the work of Bushnell et al.⁽¹⁾ for hypersonic turbulent boundary layers.

In the framework of the eddy viscosity concept, the apparent viscosity coefficient becomes

$$-\rho \langle u'v' \rangle - \langle \rho'u'v' \rangle = \rho \epsilon \left(1 + \frac{\sqrt{\rho'^2}}{\rho} \right) \frac{\partial u}{\partial y} \quad (11)$$

The turbulent Prandtl number can be defined as

$$Pr_t = \frac{\langle u'v' \rangle \left(1 + \alpha_{\rho uv} \frac{\sqrt{\rho'^2}}{\rho} \right) \left(\frac{\partial T}{\partial y} \right)}{\langle v'T' \rangle \left(1 + \alpha_{\rho vh} \frac{\sqrt{\rho'^2}}{\rho} \right) \left(\frac{\partial u}{\partial y} \right)} \quad (12)$$

In the present analysis, the turbulent Prandtl number reduces to the conventional form^(4,13) by assigning $\alpha_{\rho uv} = \alpha_{\rho vh} = 1$.

The apparent mass flux $\langle \rho'v' \rangle$ appears consistently with ρv in the same form throughout the governing equations. This term is easily taken into account by defining

$$\tilde{v} = v + \frac{\langle \rho'v' \rangle}{\rho} \quad (13)$$

The correlation term $\rho \langle v'v' \rangle$ in the normal momentum equation is closely related to the turbulent shear stress. Bradshaw has shown⁽¹⁴⁾ that the turbulent shear stress can be approximated as follows:

$$\langle u'v' \rangle = 0.15 (u'^2 + v'^2 + w'^2) \quad (14)$$

The correlation can be observed from the data of Klebanoff.⁽¹⁵⁾ A similar correlation can be observed between $\langle v'^2 \rangle$ and the turbulent kinetic energy, $(u'^2 + v'^2 + w'^2)$. According to the data of Ref. 15, the correlation:

constant appears to be about 0.2 over the major portion of the boundary layer. The profiles of $\langle u'v' \rangle / q$ and $\langle v'^2 \rangle / q$ across a turbulent boundary layer can be deduced from the data of Klebanoff⁽¹⁵⁾ and is presented in Figure 1.

$$\langle v'^2 \rangle \approx 0.2 (u'^2 + v'^2 + w'^2) \quad (15)$$

Therefore, the correlation term of $\rho \langle v'v' \rangle$ may be approximated as

$$\rho \langle v'v' \rangle = 1.4 \rho \epsilon \frac{\partial u}{\partial y} \quad (16)$$

Finally, closure of the governing equations was obtained by introducing the perfect gas law and Sutherland's viscosity equation. The Levy-Lees transformation converts the governing equations into

$$\bar{v}_\eta + 2\xi F_\xi + F = 0 \quad (17)$$

$$(C\bar{\epsilon}F_\eta)_\eta - \bar{v}F_\eta + \beta(\theta - F^2) = 2\xi FF_\xi \quad (18)$$

$$\left[\frac{\rho}{\gamma M_e^2 p_e} + 1.4 \frac{C\mu_e(\bar{\epsilon} - 1)}{(2\xi)^{1/2}} F_\eta \right]_\eta = 0 \quad (19)$$

$$\left(\frac{1}{Pr} C\hat{\epsilon}\theta_\eta \right)_\eta - \bar{v}\theta_\eta + C\bar{\epsilon}F^2_\eta = 2\xi FF_\xi \quad (20)$$

where \bar{v} is defined as

$$\bar{v} = \frac{2\xi}{\rho_e u_e \mu_e} \left[\frac{\partial \eta}{\partial x} F + \frac{\rho \bar{v}}{(2\xi)^{1/2}} \right]$$

The set of equations is identical to that of Ref. 5, except for the additional normal momentum equation, which, however, indicates that the variation of the static pressure across the turbulent boundary layer is small. The pressure variation is such that $p + \rho \langle v'^2 \rangle (1 + \sqrt{\rho'^2}/\rho)$ remains constant within the turbulent boundary layer. At the wall $\langle v'^2 \rangle$ vanishes and there the surface pressure then reaches the maximum value.

The numerical scheme used in the present analysis was identical to that of Ref. 5, except the density variation was deduced from the equation of state by

the computed temperature and pressure. The continuity equation was solved by a straightforward differencing scheme. The normal momentum equation reduced to a single algebraic equation related to the local Reynolds shear stress. The streamwise momentum equation and energy equation were solved simultaneously by an implicit scheme together with an iteration procedure of the nondimensional velocity and temperature profiles. The detailed description of the numerical method is included in Refs. 5 and 16.

SECTION III

EDDY VISCOSITY MODEL

Several multilayer viscosity models have been used successfully to predict the flow properties of compressible turbulent boundary layers.^(4,13) The differences among numerical solutions by various eddy viscosity models are small.⁽⁵⁾ The crucial point in selecting the eddy viscosity model is the damping factor in the viscous sublayer, which determines the length scale, skin friction and heat transfer. The most versatile damping factor in which the effect of mass transfer can be easily included by adjusting a constant, is due to Van Driest. In fact, Bushnell et al.⁽¹⁾ have established the correlation between the damping constant and the dimensionless blowing rate. The two-layer eddy viscosity model for the hypersonic turbulent boundary layer

can be given as

Inner region

$$\left(\frac{\epsilon}{\nu}\right)_i = \frac{k_1^2 y^2}{\nu} \left\{ 1 - \exp \left[- \frac{y}{26\nu} \left(\frac{\tau}{\rho}\right)^{1/2} \right]^2 \right\} \left| \frac{\partial u}{\partial y} \right| \left(1 + \frac{\sqrt{\rho^{1/2}}}{\rho} \right) \quad (21)$$

where k_1 is the well-known von Karman constant. In the present analysis, a value of 0.4 was used for k_1 . The inner layer model differs from that of Cebeci's work⁽⁴⁾ only in the evaluation of the shear stress in the damping factor. In the present analysis the shear stress assumes the local value instead of the wall value used in Cebeci's work. The last term in Eq. (21) is the modification for density fluctuation at hypersonic Mach numbers. The density fluctuation term also appears in the outer region of the eddy viscosity model. We have

$$\left(\frac{\epsilon}{\nu}\right)_o = \left(k_2 u_e \delta_i^* \gamma \left(\frac{y}{\delta}\right) / \nu \right) \left(1 + \frac{\sqrt{\rho^{1/2}}}{\rho} \right) \quad (22)$$

The constant k_2 is given the value of 0.0168. The quantity $\gamma(y/\delta)$ is the so called intermittency factor in the law of the wake region. The $\delta_i^* = \int_0^\delta (1-u/u_e) dy$ is the commonly accepted length scale from the velocity defect law.

The transition model of Dhawan and Harasimha⁽¹⁷⁾ was adopted in the present analysis

$$\tau = \rho(\nu + \Gamma\epsilon) \frac{\partial u}{\partial y}$$

where

$$\Gamma(\bar{x}) = 1 - \exp(-.412 \bar{x}^2)$$

The normalized streamwise coordinate in the transition region is defined as

$$\bar{x} = \frac{x - x_{t,i}}{\Lambda} \quad x_{t,i} \leq x \leq x_{t,f}$$

The parameter Λ is a measure of the extent of the transition region defined by

$$\Lambda = x_{\Gamma=3/4} - x_{\Gamma=1/4}$$

The transition model successfully described the transition behavior for the supersonic compressible turbulent boundary layer.⁽⁵⁾ The transition model requires knowledge of the beginning of the transition and the extent of the transition region. According to a substantial amount of experimental data, the Reynolds number at the end of the transition region is twice its value at the beginning of transition. This experimental observation was incorporated into the transition model. Therefore the only information required was the onset of the location of transition. For all the calculated cases, this location is contained by $1.75 \times 10^3 \leq Re_\theta \leq 2.2 \times 10^3$.

The present modification of the eddy viscosity model for extension to hypersonic flows is accomplished by including the density fluctuation term. Bushnell et al. introduced the density fluctuation term by a mixing length type model. Essential agreement between their numerical solution and hypersonic turbulent boundary layer data was obtained. Their achievement confirms the basic contention that the density fluctuation term at hypersonic speeds is significant. The density fluctuation term of the present analysis was obtained from the data of Kistler at Mach numbers up to 4.7 and for near adiabatic wall conditions. This modification was then used to perform calculations at higher Mach numbers and with heat transfer. The justification is based on the fact that the relative temperature fluctuation scaled by $2(T_0 - T_\infty)/(T_0 + T_\infty)$ is nearly independent of Mach number. Kovansnay,⁽¹⁸⁾ Kistler⁽¹¹⁾ and Laderman et al.⁽⁶⁾ have found a strong negative correlation between the temperature and the velocity fluctuation $\langle u'T' \rangle$. The static temperature fluctuation levels are proportional to the temperature difference across the boundary layer.⁽¹¹⁾ Further, the temperature fluctuation level obtained by Laderman and Demetriades for a highly cooled wall at a Mach number of 9.37 was similar to the data of Kistler, although at a lower value.

From the equation of state, the fluctuating thermodynamic properties can be expressed as

$$\frac{p'}{p} = \frac{\rho'}{\rho} + \frac{T'}{T}$$

The temperature fluctuations obtained by Kistler⁽¹¹⁾ were based on the assumption that the pressure fluctuation is negligible. Thus the temperature and density fluctuations are identical in magnitude but opposite in sign. This equality, which also has been pointed out by Laufer,⁽¹⁹⁾ is not a direct result of measurement.

In the present analysis, a pressure fluctuation term has been obtained from the normal momentum Eq. (3). The origin of this pressure variation is attributed by the normal component of the Reynolds shear stress. The correlated pressure variation is proportional to $\gamma M_e^2 (2\tau/\rho u^2)$. It is interesting to note that the present result is almost identical to the experimental result of Kistler et al.⁽⁸⁾ They estimated the relative level of the pressure fluctuation to be $\langle p \rangle / p \approx 2.5 M_e^2 C_f$ for $M_e > 2$. Further, Laderman and Demetriade⁽²²⁾ have shown that the relative magnitude of the density fluctuation is greater than that of the pressure and temperature fluctuation. In order to be consistent with the present formulation, the RMS value of the density fluctuation is tentatively given as

$$\frac{\sqrt{\rho'^2}}{\rho} = \frac{\sqrt{T'^2}}{T} + \frac{\langle (\rho v)' v' \rangle}{p} \quad (23)$$

The RMS value of the temperature fluctuation is introduced as

$$\frac{\sqrt{T'^2}}{T} = 2 \left(\frac{T_0 - T_\infty}{T_0 + T_\infty} \right) f \left(\frac{y}{\delta} \right) \quad (24)$$

where $f(y/\delta)$ gives a fitting of Kistler's data, having a maximum value of 0.1. The pressure fluctuation term was calculated from the normal momentum equation.

SECTION IV
TURBULENT PRANDTL NUMBER

Recently Simpson et al.⁽¹⁰⁾ have established the uncertainty envelope of the turbulent Prandtl number for incompressible zero pressure gradient turbulent boundaries. They conclude that in the wall region the molecular viscosity, Prandtl number and the small scale turbulence govern the momentum and heat transport. Furthermore, the turbulent Prandtl number is greater than unity at the wall. However, in the outer region Pr_t is less than unity. Several turbulent Prandtl number models have been developed.^(9,10) The most common characteristic is that the predicted Pr_t value exceeds unity near the wall. The maximum value of Pr_t seems to be 1.35 at the wall. Experimental data by Meier and Rotta at Mach numbers up to 4.5 and near adiabatic wall conditions yield a Pr_t distribution with a value greater than unity near the wall. Data by Horstman and Owen⁽²⁰⁾ at $M_e = 7.2$ and cooled wall conditions also indicate this behavior. Nevertheless, all the predictions fall into the uncertainty envelope of Simpson et al. In view of the unresolved question on the Pr_t , an empirical Pr_t distribution has been suggested by Rotta⁽²¹⁾ as follows:

$$Pr_t = .95 - 0.45 (y/\delta)^2$$

This appears to be a very good approximation of the Pr_t in the outer region. For the purpose of studying the sensitivity of Pr_t on the present numerical solutions, a similar empirical formulation is suggested as follows:

$$Pr_t = Pr_1 e^{-10(y/\delta)} + Pr_2 \left[1 - 0.2 \left(\frac{y}{\delta} \right) \right] \quad (25)$$

where $0.8 \leq Pr_2 \leq 1.0$, $.2 \leq Pr_1 \leq .4$.

The above approximation closely follows the outer bounds of the data. If Pr_2 is assigned to be 0.90, $Pr_1 = 0.30$, the Pr_t distribution by Eq. (25) describes approximately the mean value of the uncertainty envelope. A graphical presentation of the uncertainty envelope of the turbulent Prandtl number and the present approximations of its limits are given in Figure 2.

SECTION V

DISCUSSION OF RESULTS

The computed results are presented in three sections. The first portion of the results is concerned with the pressure variation due to turbulence across the hypersonic turbulent boundary layer and its influence on the characteristics of the shear layer. The second section of the presentation is an evaluation of the turbulent heat flux in terms of the Prandtl number variation. This parameter is a measure of the relative magnitude between the eddy viscosity and the apparent heat conductivity $Pr_t = C_p \rho \epsilon / \lambda_t$. The remaining section is devoted to the solution of hypersonic turbulent boundary layers with the inclusion of the density fluctuation terms. The validity of this eddy viscosity model in the hypersonic flow regime with heat transfer is determined by means of comparison with experimental data.

The third figure presents the static pressure variation across the turbulent boundary layer at Mach number 9.37. The experimental data were obtained by Laderman and Demetriades.⁽⁶⁾ The normalizing boundary layer thickness in the presentation of their data is considered to be 4.4 inches according to their revised value.⁽²²⁾ The calculated pressure distribution within the boundary layer agrees very well with the measurement. The pressure decreases very rapidly from the wall, reaches the minimum value near the outer edge of the sublayer, and then approaches the free stream value asymptotically. The pressure variation across the turbulent boundary is directly proportional to the turbulent shear stress distribution. The relative magnitude of the pressure variation is proportional to the square of the free stream Mach number and the correlation function between $\langle v'^2 \rangle$ and the turbulent kinetic energy. The present modeling of the pressure variation assumed no free stream turbulence. Therefore the surface pressure equals the free stream value. If the free stream turbulence value can be assessed, the maximum pressure will be attained at the surface as that reported by Fischer et al.⁽⁷⁾

In order to evaluate the significance of the small pressure variation on the mean motion, calculations were performed with and without the inclusion of the pressure fluctuation term. The difference between the two calculations is negligible for the cases investigated. In addition, a reduction in streamwise step size for the numerical scheme must be implemented to include the normal momentum equation. In spite of the small transverse pressure variation, the numerical procedure required a significantly large number of iterations to meet the established convergent criterion. The solution even failed to converge if too coarse a streamwise mesh size were assigned. Based upon the aforementioned observations, the small pressure variation across the

turbulent boundary layer was neglected in the mean equation of motion in the following analysis.

To examine the influence of turbulent Prandtl number on numerical solutions, an empirical formulation of the turbulent Prandtl number was introduced. The empirical expression provided a close description of the upper and lower limits of the uncertainty envelope of the turbulent Prandtl number. The molecular Prandtl number was assigned the value of 0.73 throughout the test. Holden's data⁽²³⁾ of the skin friction coefficient and Stanton number were used for the evaluation process. His turbulent flow data were taken under a natural laminar-turbulent transition condition.

Figure 4 presents the skin friction coefficient and Stanton number distributions at $M_e = 7.97$ with a wall to free stream stagnation temperature ratio of $T_w/T_0 = 0.308$. Two numerical solutions are presented in the graph. One of the solutions is computed by assuming the upper limit of the Prandtl number variation, and the other assumes the lower limit. In the present context, the Pr_t distributions across the boundary layer were generated from Eq. (25). The upper limit of the Pr_t variation is obtained by assigning $Pr_1 = 0.4$ and $Pr_2 = 1.0$; the lower limit of the Pr_t variation is calculated with $Pr_1 = 0.2$ and $Pr_2 = 0.8$. The difference in the boundary layer calculations was found to be small. The computed Stanton number and skin friction coefficient distributions indicate excellent agreement with the experimental data. The difference between the two solutions is noticeable downstream of the transition region. The solution associated with the upper limit Pr_t variation yields a lower value of C_f than the solution by the lower limit Pr_t . However, the trend is reversed in predicting the Stanton number. As a consequence, the Reynolds analogy factor $2St/C_f$ is decreased with decreasing

turbulent Prandtl number. The identical observation can be made in the work of Bushnell and Beckwith.

The influence of turbulent Prandtl number on the detailed flow field was also investigated for the two limits of Pr_t distributions. The computed velocity profiles are nearly identical, thus only static temperature profiles are presented in Figure 5. The comparison between the data of Laderman et al.⁽⁶⁾ and the computed results is fair. One observes that the present calculations predict correctly the location of the maximum temperature in the turbulent boundary layer. The peak temperature is located near the outer edge of the viscous sublayer. The difference between the two solutions of the limiting Prandtl number distributions is small. Significant differences between the two solutions appear only in the magnitude of the maximum temperature and in the law of the wake region.

Calculations with a constant Pr_t value of 0.9 and the Pr_t distribution suggested by Rotta⁽²¹⁾ have also been performed. The calculations are contained within the limiting solutions in either C_f , St or velocity and static temperature profiles. In particular, the small difference (less than 3%) between solutions of $Pr_t = 0.9$ and Rotta's Pr_t distribution indicates an insensitivity of the numerical solutions to the Pr_t variation in the law of the wake region.

In order to ascertain the predicted trend of the skin friction and the Stanton number due to different values of Pr_t , two additional calculations with constant turbulent Prandtl numbers of 0.7 and 1.3 at $M_e = 10.57$ have been included in the present study. In Fig. 6, the calculated velocity and temperature profiles at different but constant turbulent Prandtl numbers are presented. One observes that the velocity profile is hardly affected by the

different magnitude of the constant turbulent Prandtl number. On the other hand, significant disparity in temperature profiles is obvious. The maximum deviation between two solutions appears in the magnitude of the predicted peak temperature and the temperature profile in the law of the wake region. This behavior is also perceptible in Fig. 5 for variable Pr_t distributions at different values. The calculation by the higher Pr_t value yields a higher static temperature than the calculation with a lower value of Pr_t in the laminar sublayer region. As a consequence, the calculation by the higher value of turbulent Prandtl number generates a lower eddy viscosity for the entire inner region (Figure 7). Therefore, the solution with $Pr_t = 1.3$ yields a higher heat transfer rate but lower shear stress at the wall than the solution with $Pr_t = 0.7$. In all, the Stanton number and the skin friction coefficient exhibit a relative insensitivity with respect to the turbulent Prandtl number variation. The difference of 46% in Pr_t produces a difference of only 7% in the Stanton number and 4% in C_f .

The conventional comparison of $(H-H_w)/(H_e-H_w)$ vs u/u_e is given in Fig. 8 with the data of Laderman and Demetriades for $M_e = 9.37$. In these coordinates Crocco's relationship for $Pr_t = Pr = 1$ is a straight line which is verified by the present calculation. The lower value of Pr_t in the present calculation produces a profile closer to the quadratic law than the higher value of Pr_t . The discrepancy between the data and the present calculation may be attributed to the aspect of flow history. The deviation from the Crocco relationship has been documented for data^(1,3) obtained from wind tunnel walls. Unfortunately, detailed upstream flow conditions are not available, and, hence, it is not possible to verify this contention.

In Fig. 9, the evaluation of the present eddy viscosity model with an explicit density fluctuation dependence was presented together with the data by Holden and the data by Hopkins et al. The experimental data were obtained at a Mach number of about 7.4 and T_w/T_0 from 0.172 to 0.418. All data were obtained under natural laminar to turbulent transition conditions. Holden's data of the Stanton number provided a distinctive onset location of the transition zone. Two numerical solutions consistent with the transition condition were obtained. The third calculation was obtained by assigning transition at the origin. The present eddy viscosity model which includes the density fluctuation terms predicts very well the skin friction coefficient. The conventional eddy viscosity model without the density fluctuation correction underpredicts C_f in the low Re_θ region but improves steadily downstream of the transition zone. The calculated Stanton number uniformly overpredicts the data of Holden. The difference between solutions of the eddy viscosity model without the density fluctuation correction and the present model is 7%. The turbulent Prandtl number used in these calculations was assumed to have a constant value of 0.9. This simplification was made in the present calculations so that a consistent comparison could be achieved with several other investigations. (1,2,4)

Similar comparisons at Mach number around eight are presented in Figure 10. Excellent agreement is indicated between the heat transfer data of Holden and the present calculations in the regions of laminar, transition and turbulent flows. The eddy viscosity model with the density fluctuation correction underpredicts the data of Hopkins et al. in the low Re_θ region. The eddy viscosity model without the density fluctuation correction would underpredict the data further by 8%. Agreement between the data and the

calculated C_f by the eddy viscosity model with the density fluctuation correction is nearly attained in the higher Re_θ region. The solution by the eddy viscosity model without the density fluctuation correction slight underpredicts the C_f and St measured values in the higher Re_θ region.

In Fig. 11, the calculations are compared with the data of Holden at a free stream Mach number around ten and T_w/T_0 about 0.2. The numerical solution by the eddy viscosity model without the density fluctuation correction underpredicts the skin friction coefficient over the complete range of Re_θ . These calculated heat transfer rates show better comparison with the measured results than that by the eddy viscosity model with the density fluctuation correction. However, the prediction of the heat transfer in the laminar and transitional regions is excellent. The eddy viscosity model with the density fluctuation correction yields essential agreement with the C_f measurements over the entire range of Re_θ . An interesting observation may be noted in Fig. 11; i.e., turbulent boundary layers at low Reynolds numbers, exhibit relatively high values of the shear stress and heat transfer at the wall. This phenomena can be detected for all the cases investigated. The behavior is particularly noticeable by comparing the data and the solution with an eddy viscosity model with the density fluctuation correction. The numerical solution always underpredicts C_f and St for the lower Re_θ region but reaches near agreement at the higher Re_θ region. The phenomenon is progressively more pronounced as the free stream Mach number increases.

In Fig. 12, the calculations by an eddy viscosity model with and without the density fluctuation correction are compared with the data by Holden. His data were obtained at $M_e = 12.04$ and $T_w/T_0 = 0.157$. The maximum value of Re_θ for the experiment is 6.849×10^3 . The prediction in heat transfer

is again excellent in the laminar and transition regions. Near agreement is also attained in the turbulent region. The skin friction coefficient calculation is also underpredicted in this relatively low Re_θ region. The calculation with the eddy viscosity model without the density fluctuation correction further underpredicts by 10%. To substantiate the present results, those of Van Driest's theory are also presented in Figure 12. The difference between the predictions of Van Driest theory and the present model with the density fluctuation correction is small. The measured C_f data indicate a higher value than both calculations in the low Re_θ region.

A summary of the eddy viscosity model with the density fluctuation correction over a wide range of the free stream Mach number is presented in Figure 13. Van Driest's theory suggested by Hopkins et al.⁽²⁾ is adopted to be used as the criterion. The comparison is divided into two groups. The first group is restricted to Re_θ less than 10^4 , while the second group of comparisons is presented for Re_θ greater than 10^4 . The division of Re_θ in the present comparison is rather arbitrary. The noticeable underprediction of C_f in the low Re_θ region is obvious. The difference between solutions by the eddy viscosity model without the density fluctuation correction and the present model with density fluctuation correction diminishes as the free stream Mach number decreases. The difference becomes negligible as the Mach number reaches a value less than two. This behavior is expected because the density fluctuation correction is proportional to $T_0 - T_e$. The difference between the Van Driest theory and the present calculation is small, (in general, both underpredict C_f in the lower Re_θ region) but is within the scattering of the measurements in the higher Re_θ region.

The particular behavior of the turbulent boundary layer at low Reynolds numbers has been investigated by Huffman and Bradshaw.⁽²⁴⁾ They suggested that a turbulent-irrotational interface exerts a significant effect on the outer region of a boundary layer at low Reynolds numbers. They also indicated that one of the primary effects of external influences on the inner layer is a change in the damping constant A . In Fig. 14, the dependence of the skin friction coefficient C_f on the damping constant A is presented. The original value of A in the Van Driest damping factor is 26. A value range of A from 0.01 to 99 is computed. In the present numerical procedure, the smaller value of A is equivalent to letting the damping factor D approach unity. Thus, the law of the wall is extended closer to the surface. On the other hand, the greater value of A yields a value of C_f which approaches that of the laminar flow. In this given value range of A , the calculated C_f varies by a factor of three. The deficiency in predicting C_f at the lower Re_θ region can be easily corrected by either adjusting the sublayer thickness through the damping constant or by removing the intermittency correction in the law of the wake region.⁽¹¹⁾ However, the understanding of the phenomenon can be obtained only by extensive experimental investigations.

SECTION VI

CONCLUDING REMARKS

Numerical solutions to the mean equations of turbulent motion were obtained by a finite-difference scheme. Models of the terms for the Reynolds stress and the turbulent energy flux were modified to include the effect of fluctuating density which becomes significant at hypersonic speeds. The influence of the turbulent Prandtl number on a numerical solution was also investigated.

The present eddy viscosity model with an explicit dependence on the density fluctuation term predicts the skin friction coefficient and the heat transfer at hypersonic Mach numbers. The agreement between data and the calculations is excellent in the laminar and transition regions. In the turbulent flow regime, the present solutions as well as all current theories underpredict the skin friction data in the lower Re_θ region. However, the accuracy improves steadily as the flow proceeds farther downstream of the transition region. In the higher Re_θ region, the agreement between the data and the present solutions is excellent. On the other hand, the eddy viscosity model without the density fluctuation correction significantly underpredicts the skin friction coefficient data. The discrepancy between data and calculations without the fluctuating density correction becomes progressively more pronounced as the free stream Mach number increases. The density fluctuation correction term seems to be necessary to improve the accuracy of solutions in the investigated hypersonic flow regime.

The present analysis indicates that in a turbulent boundary layer the sum $p + \langle(\rho v)'v'\rangle$ remains constant across the shear layer. Therefore the static pressure across the boundary layer must adjust itself to accommodate

the fluctuating transverse velocity term. According to the present model, the maximum magnitude of the velocity fluctuation term is about five percent of the free stream static pressure value at $M_e = 9.37$. The corresponding static pressure reaches the minimum value near the outer region of the laminar sublayer. The effect of this pressure variation is negligible for the investigated cases, however.

The numerical solutions exhibit a weak dependence on the turbulent Prandtl number variation. For turbulent Prandtl numbers differing by more than 40%, calculations show merely a 6% difference in C_f and Stanton number. The Reynolds analogy factor, $2St/C_f$ was between 0.9 and 1.0 for these cases. These encouraging numerical computations show that the density fluctuation correction improves the overall accuracy of the solutions in the hypersonic flow region.

$$q = (U'^2 + V'^2 + W'^2)$$

DATA OF KLEBANOFF ¹⁵

⊙ $\langle U'V' \rangle / q$
 ⊠ $\langle V'^2 \rangle / q$

$\langle U'V' \rangle / q$
 $\langle V'^2 \rangle / q$

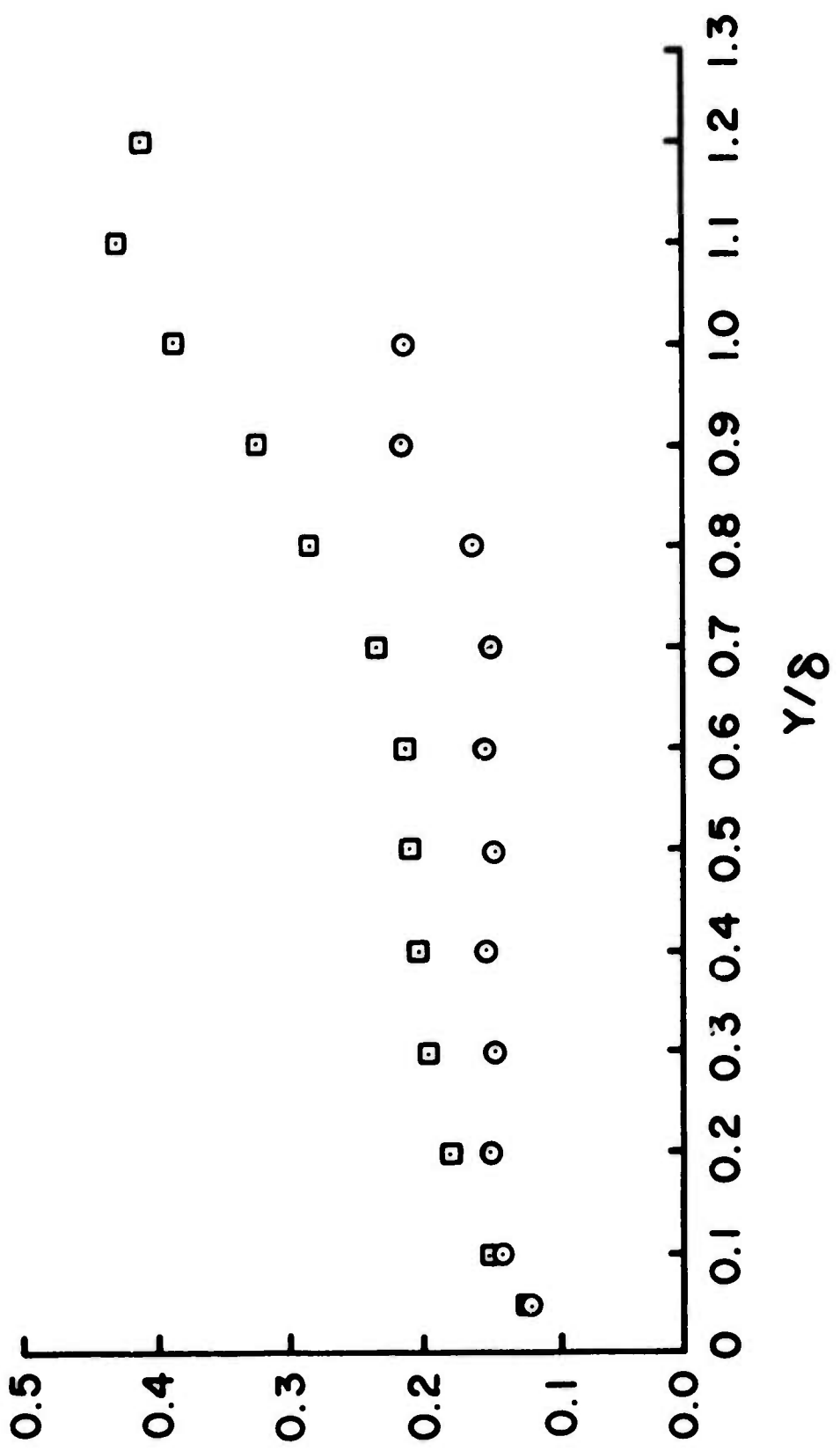


FIGURE 1 Correlation of the Turbulent Kinetic Energy, the Reynolds Shear Stress and ...

UNCERTAINTY ENVELOPE¹⁰

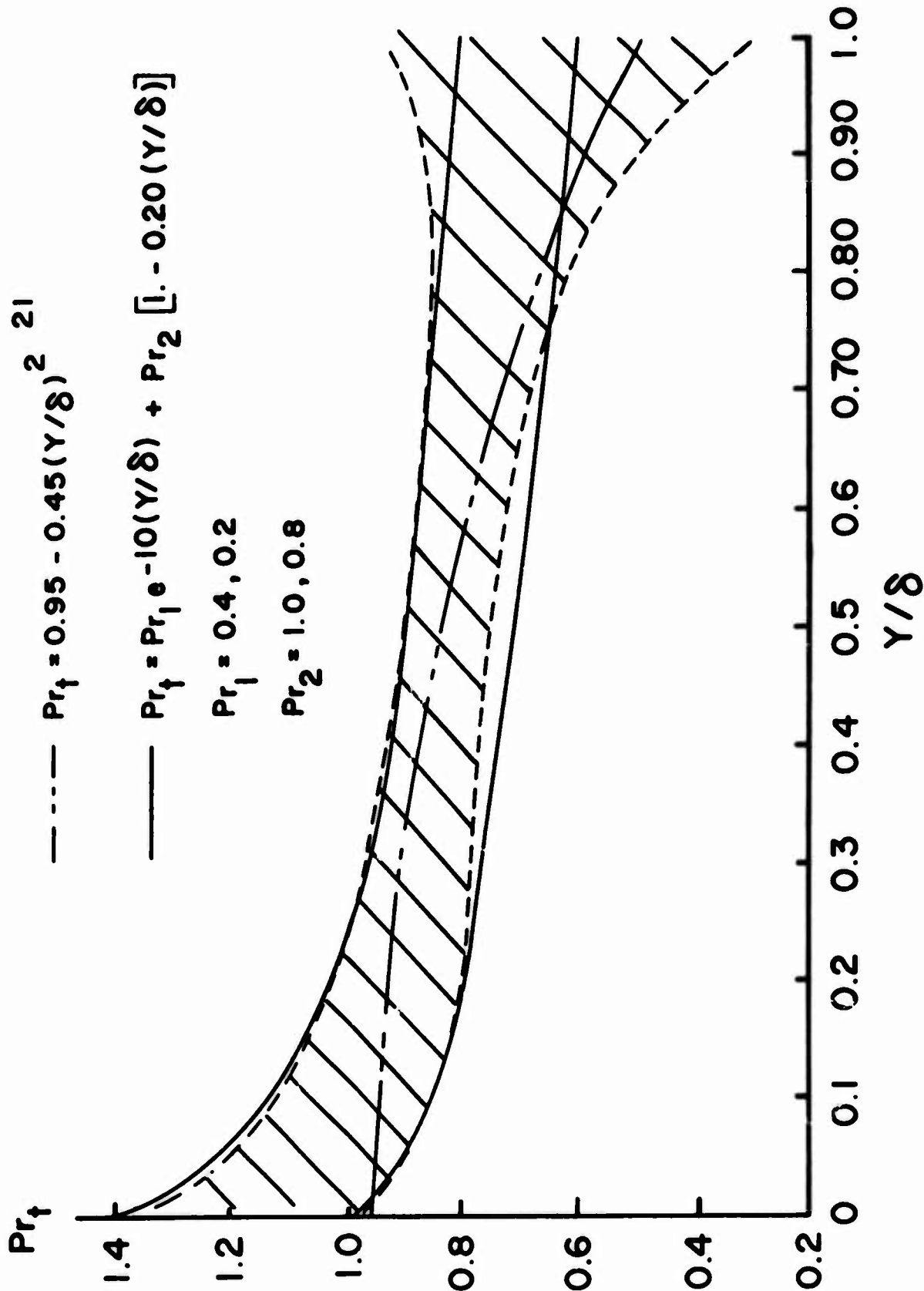


FIGURE 2 The Uncertainty Envelope of the Turbulent Prandtl Number and the Approximated Pr_t Distributions

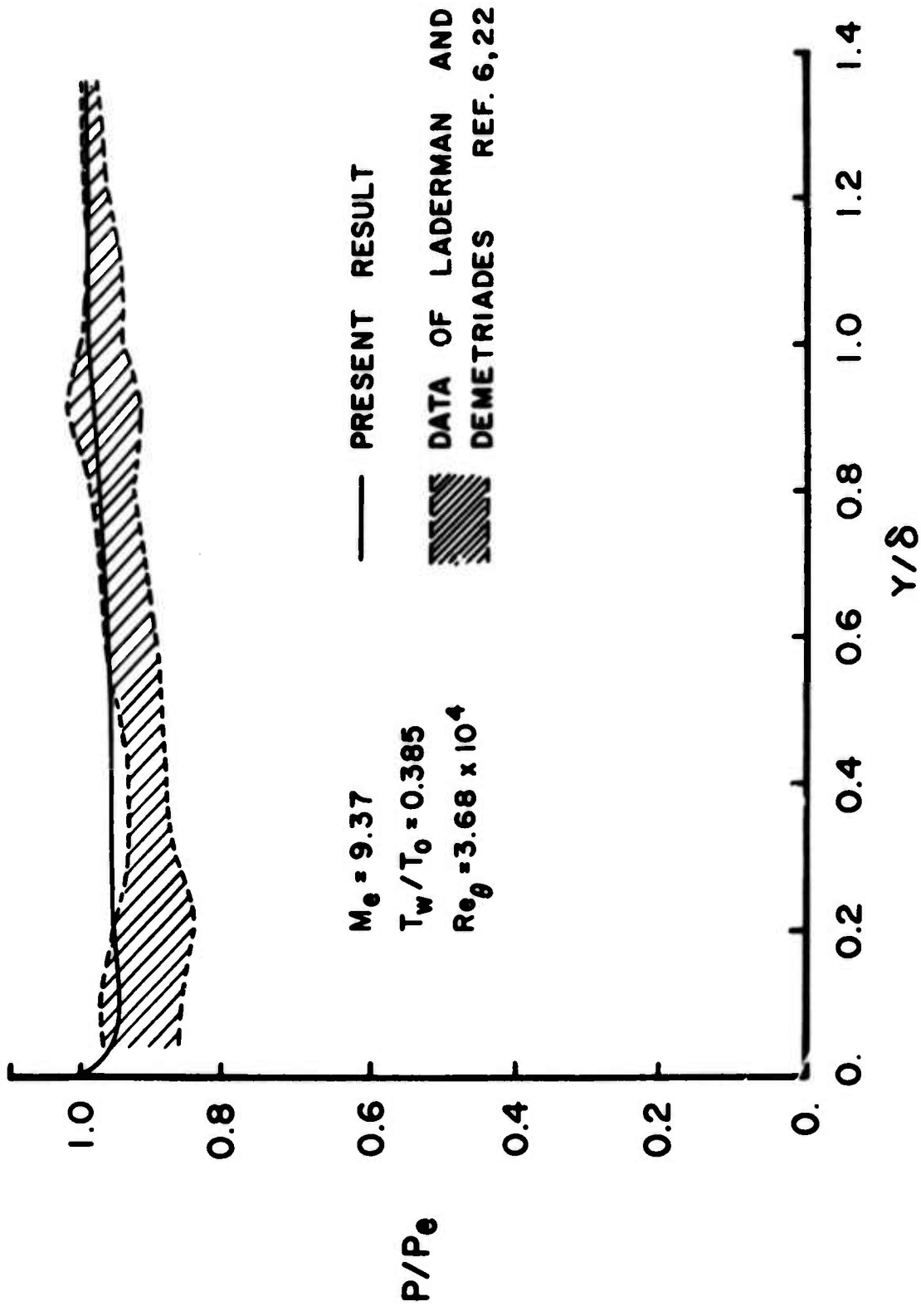


FIGURE 3 Static Pressure Distribution Across Turbulent Boundary Layer

$$----- Pr_{\dagger} = 0.4 e^{-10(Y/\delta)} + (1.0 - 0.20(Y/\delta))$$

$$-+- Pr_{\dagger} = 0.2 e^{-10(Y/\delta)} + 0.8(1. - 0.20(Y/\delta))$$

| DATA | M_{∞} | T_w/T_0 |
|------|--------------|-----------|
| ○ | 7.97 | 0.3076 |
| □ | 7.982 | 0.2692 |

HOLDEN 23

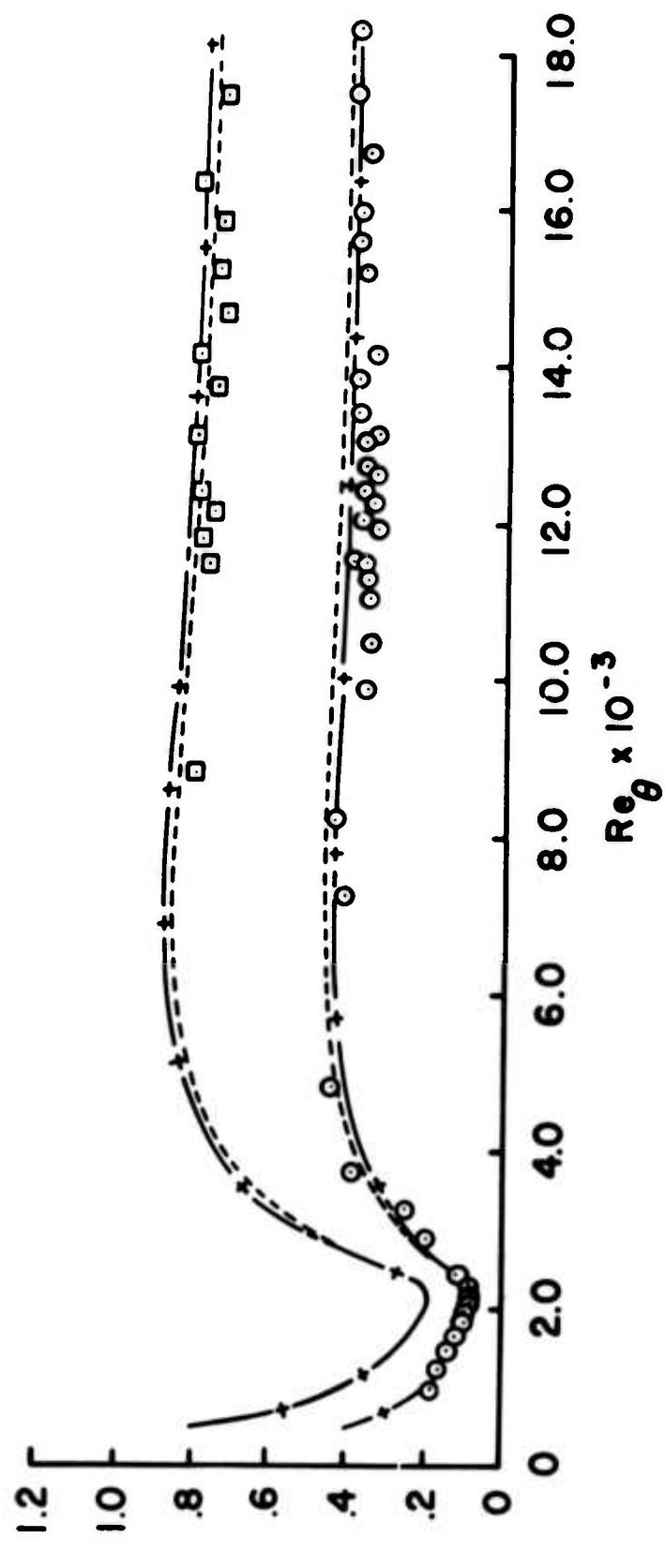


FIGURE 4 Effect of Variable Turbulent Prandtl Number on C_f and St

$$M_e = 9.37 \quad T_w/T_o = 0.385 \quad Re_\theta = 3.68 \times 10^4$$

□ DATA OF LADERMAN & DEMETRIADES⁶

$$+ \text{---} + Pr_\dagger = 0.2 e^{-10(Y/\delta)} + 0.8(1 - 0.2(Y/\delta))$$

$$\text{-----} Pr_\dagger = 0.4 e^{-10(Y/\delta)} + 0.8(1 - 0.2(Y/\delta))$$

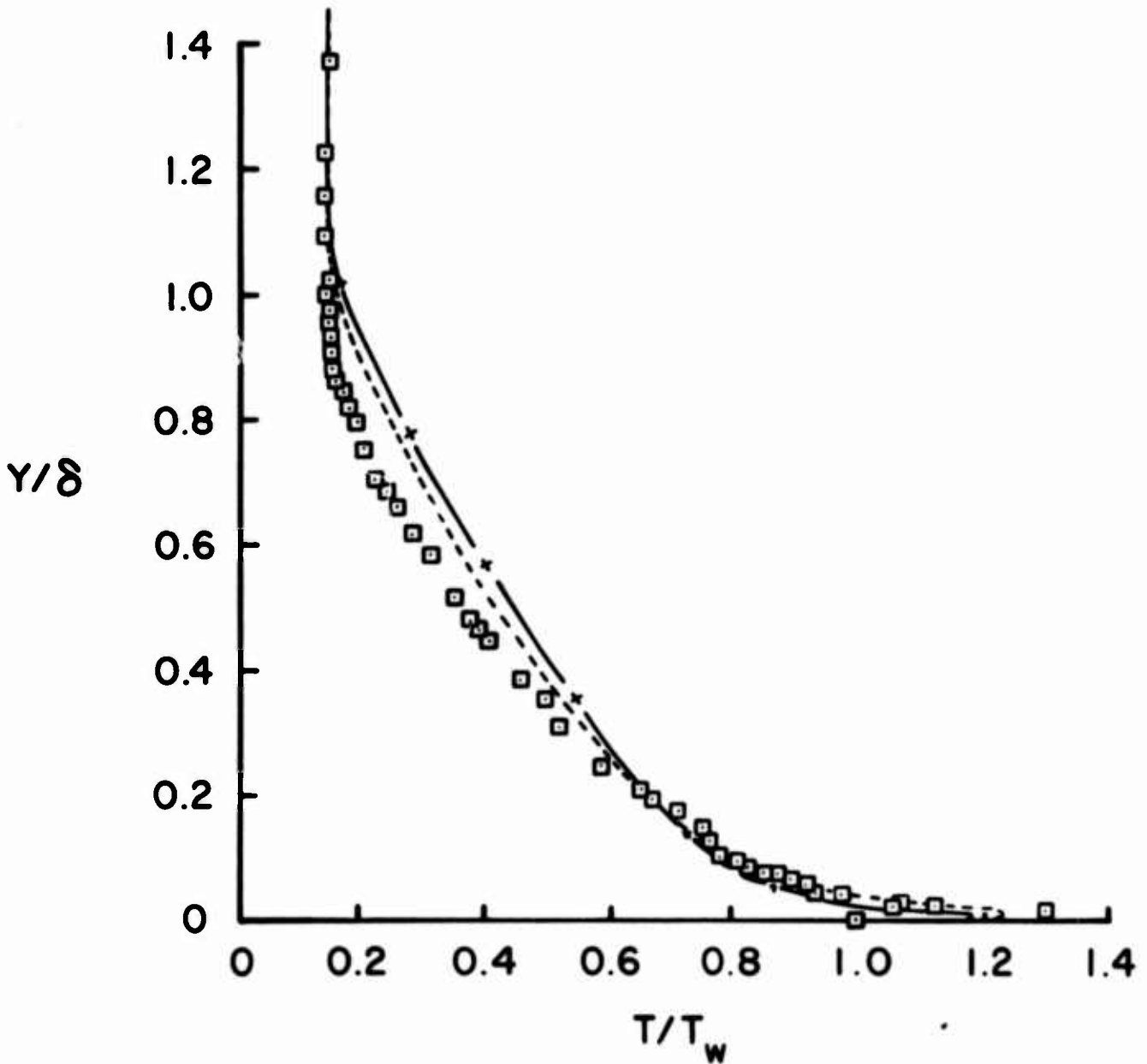


FIGURE 5 Effect of Variable Turbulent Prandtl Number on Temperature Profile

$$Me = 10.57 \quad T_w/T_0 = .2012 \quad Re_x = 4.76 \times 10^7$$

$$\text{---+---} \quad Pr_t = 0.7 \quad C_f = .5971 \times 10^{-3} \quad S_f = .2885 \times 10^{-3}$$

$$\text{---} \quad Pr_t = 1.3 \quad C_f = .5555 \times 10^{-3} \quad S_f = .3121 \times 10^{-3}$$

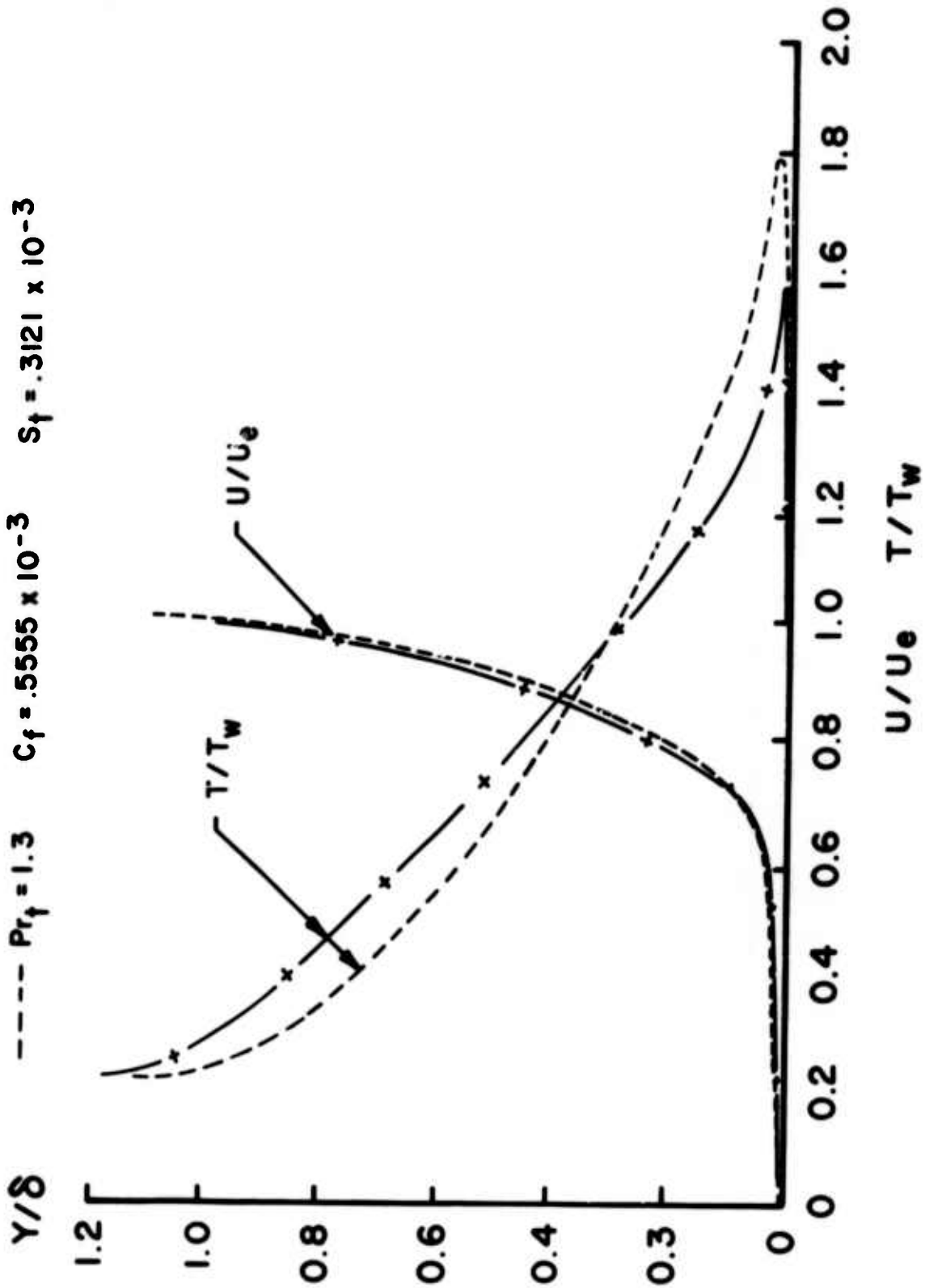


FIGURE 6 Effect of Constant Turbulent Prandtl Number on Temperature and Velocity Profiles

$M_0 = 10.57$ $T_w / T_0 = 0.2012$ $Re_x = 4.76 \times 10^7$

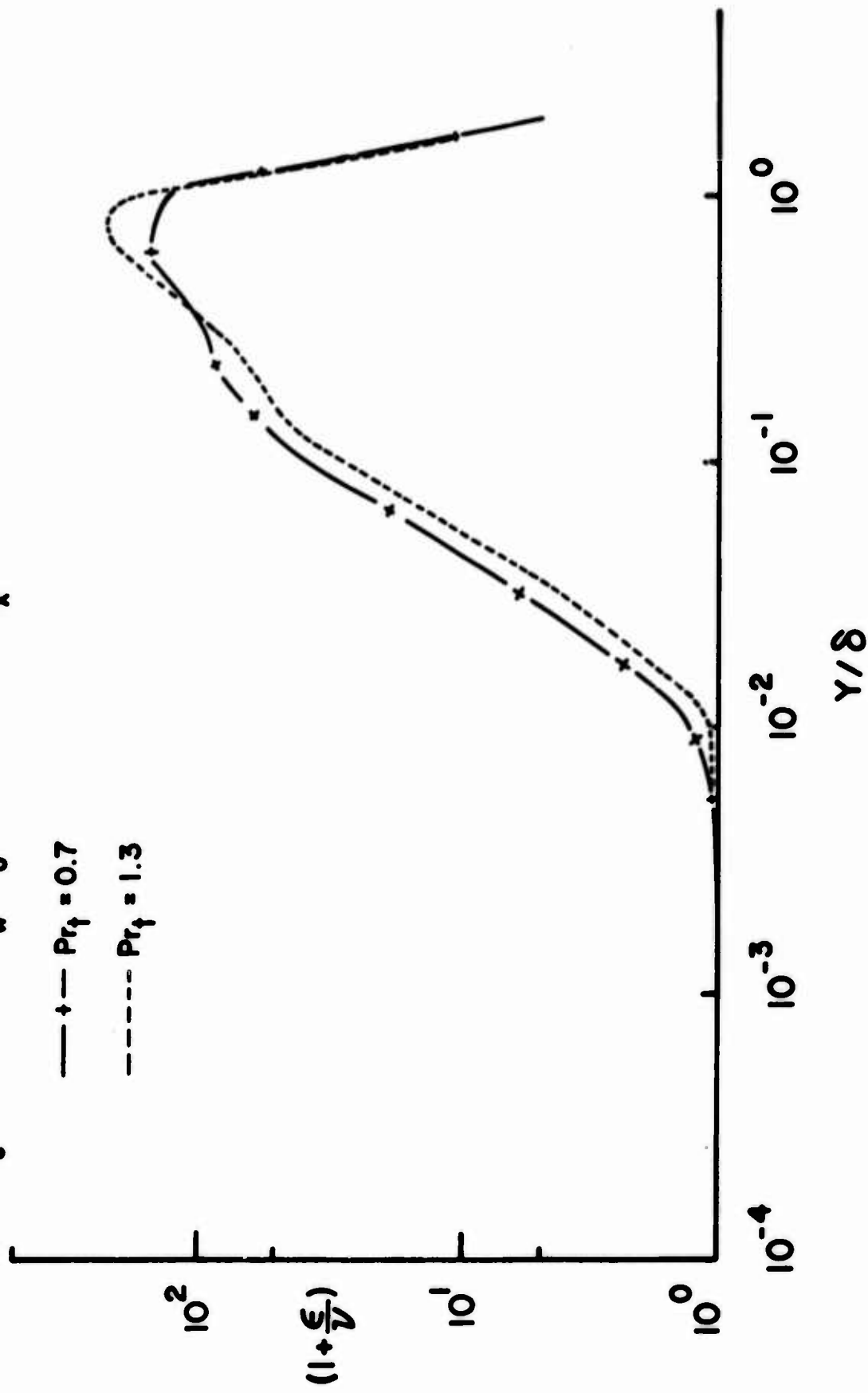


FIGURE 7 Effect of Constant Turbulent Prandtl Number on the Eddy Viscosity Coefficient Distribution

$M_e = 9.37$ $T_w / T_0 = .385$ $Re_\theta = 36,900$

○ DATA OF LADERMAN & DEMETRIADES⁶
 CALCULATIONS

- $Pr = 1.0$ $Pr_\dagger = 1.0$
- $Pr = 0.73$ $Pr_\dagger = .4e^{-10(Y/\delta)} + (1 - 0.2(Y/\delta))$
- +- $Pr = 0.73$ $Pr_\dagger = .2e^{-10(Y/\delta)} + 0.8(1 - 0.2(Y/\delta))$

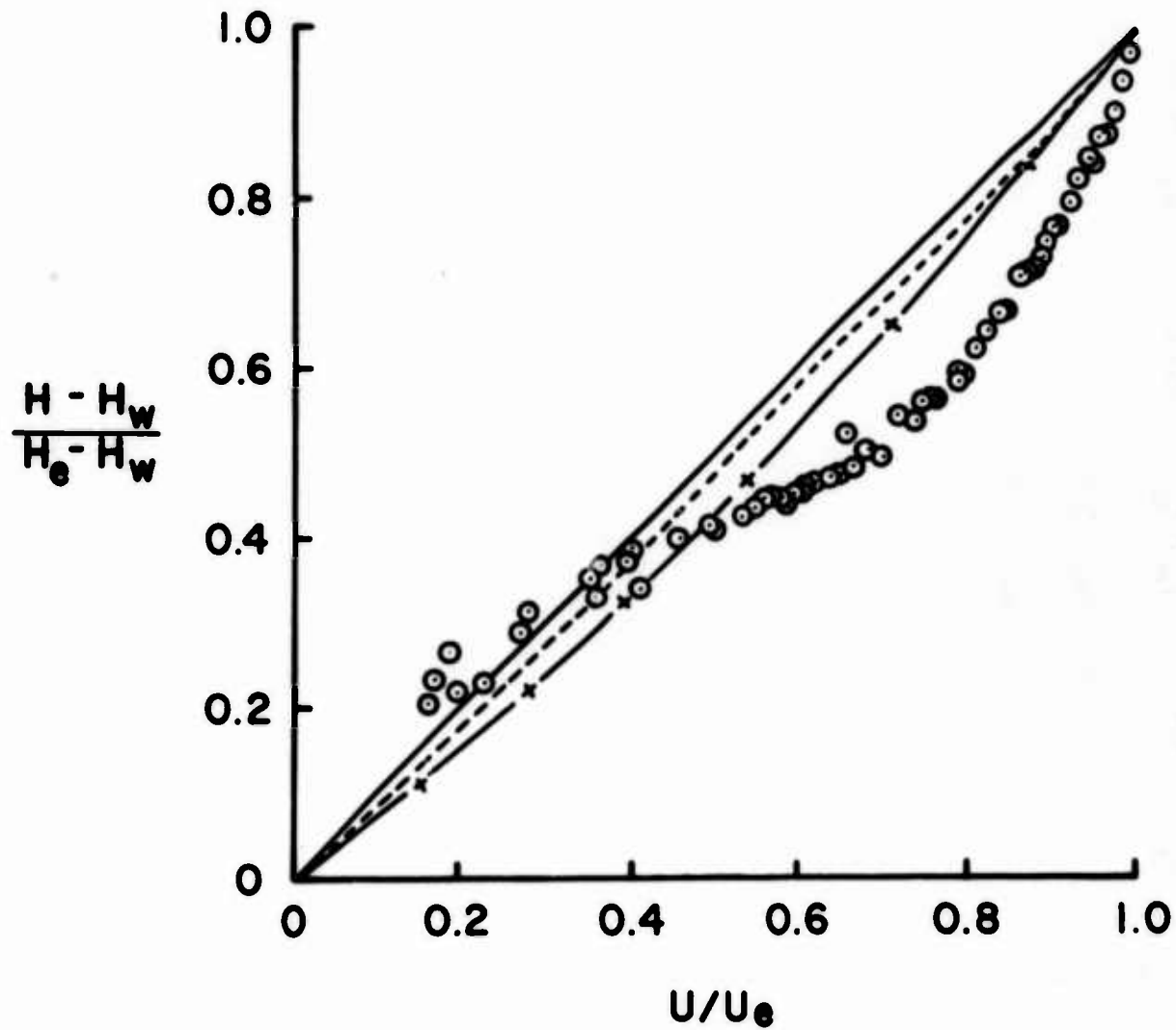


FIGURE 8 Nondimensional Total Enthalpy Versus Velocity

$$\begin{cases} \text{---} \tau_{\dagger} = - [\rho \langle u'v' \rangle + \langle \rho' u'v' \rangle] \\ \text{---} \tau_{\dagger} = - \rho \langle u'v' \rangle \end{cases}$$

$$Pr_{\dagger} = 0.9$$

| DATA | M_e | T_w / T_0 |
|------|-------|-------------|
| ○ | 7.367 | 0.172 |
| □ | 7.4 | 0.418 |
| ○ | 7.4 | 0.265 |

HOLDEN 23

HOPKINS et al 2

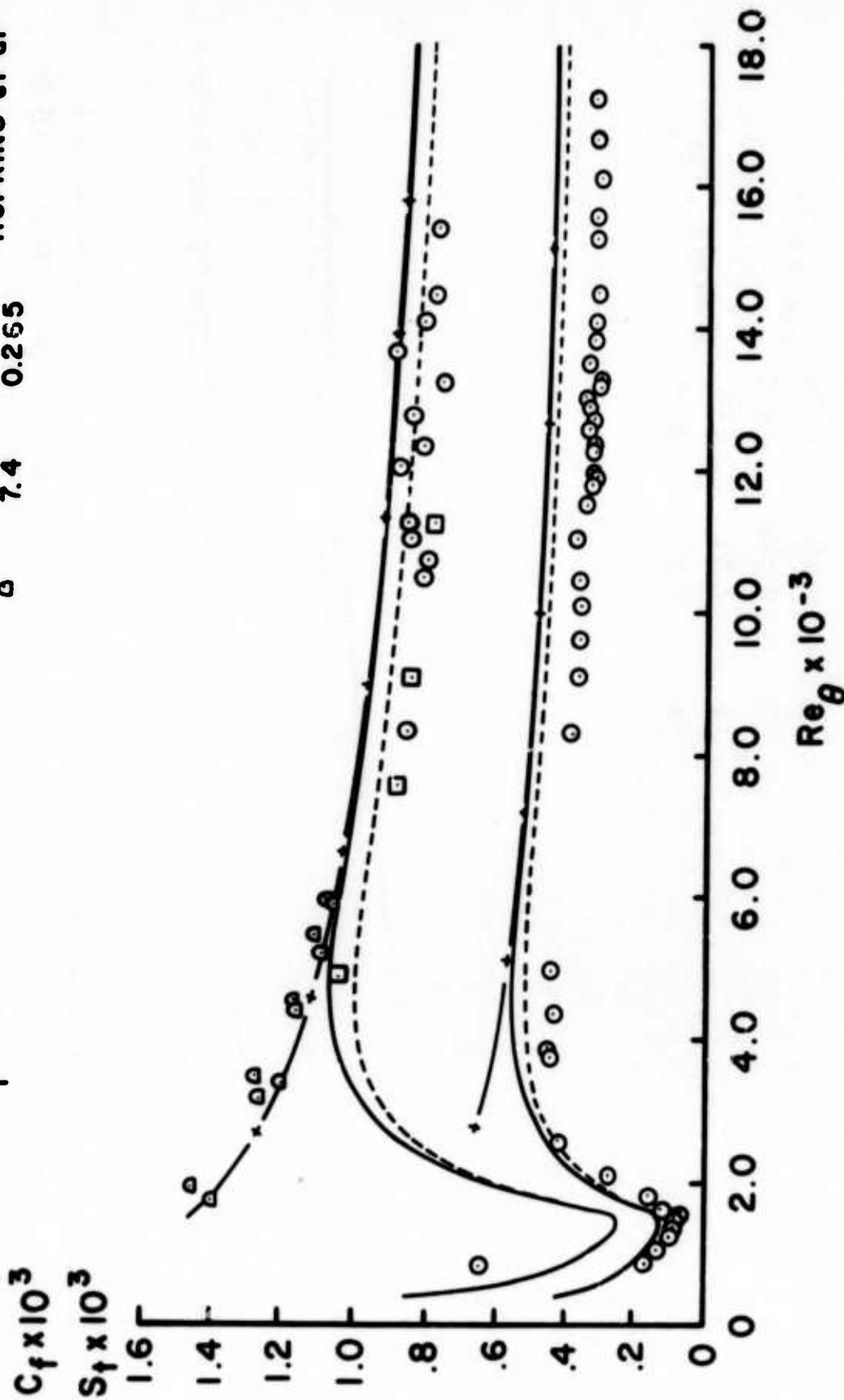


FIGURE 9 Effect of Density Fluctuation on C_f and St at $M_e = 7.4$

$$\left. \begin{array}{l} \text{---+---} \\ \text{---} \\ \text{---} \end{array} \right\} \tau_f = -[\rho \langle u'v' \rangle + \langle \rho' u'v' \rangle]$$

$$\text{---} \tau_f = -\rho \langle u'v' \rangle$$

$$Pr_f = 0.9$$

| DATA | Me | T_w/T_0 |
|------|-------|-----------|
| ○ | 7.97 | .3076 |
| □ | 7.982 | .2692 |
| △ | 7.70 | .276 |
| ● | 7.80 | .445 |

HOLDEN 23

HOPKINS et al²

$C_f \times 10^3$
 $St \times 10^3$

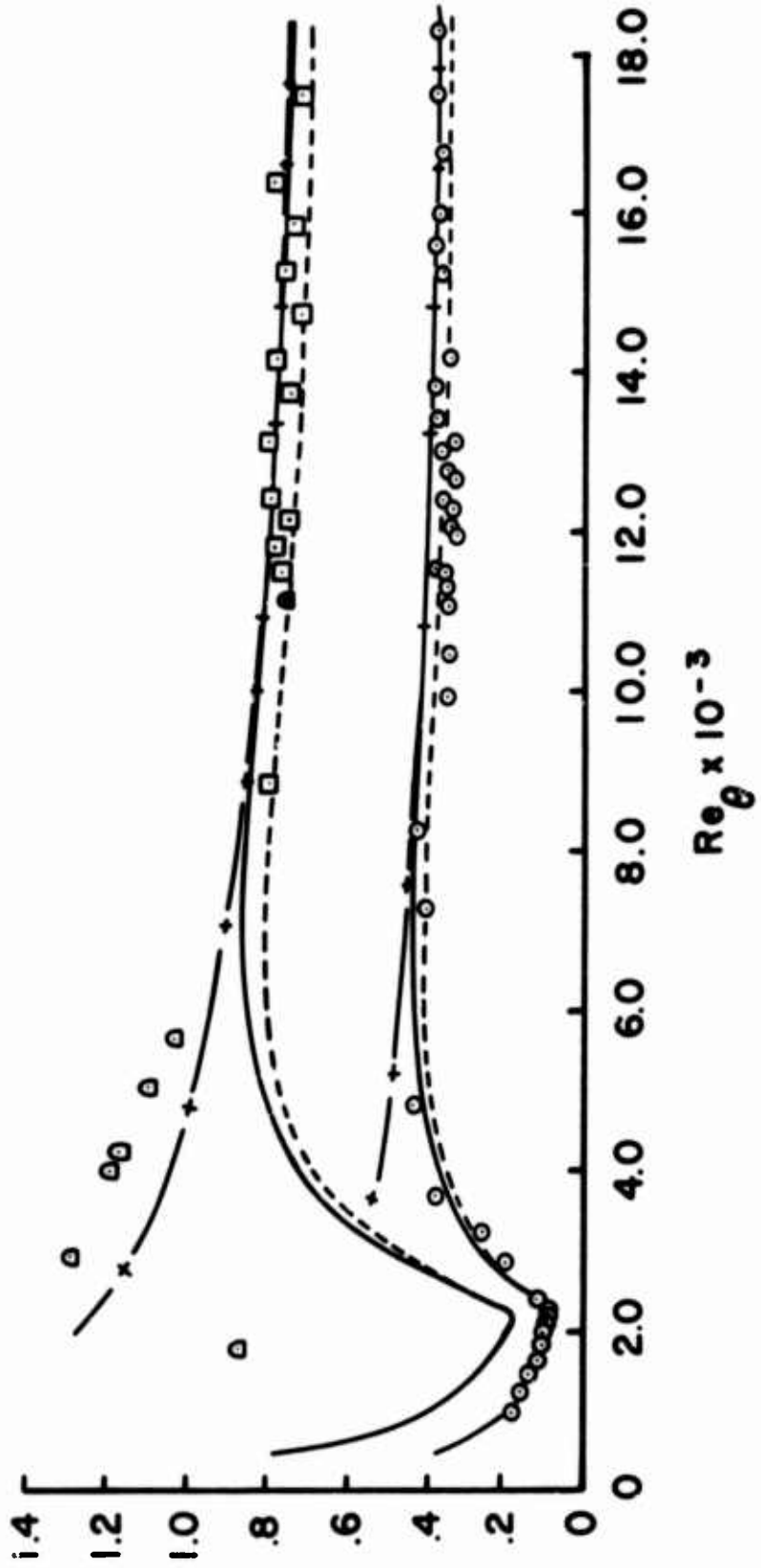


FIGURE 10 Effect of Density Fluctuation on C_f and St at $He \approx 8.0$

$\tau_f = - [\rho \langle u'v' \rangle + \langle \rho' u'v' \rangle]$
 $\tau_f = - \rho \langle u'v' \rangle$
 $Pr_f = 0.9$
 HOLDEN 23

| DATA | M_e | T_w/T_0 |
|------|-------|-----------|
| ○ | 10.72 | .194 |
| □ | 10.57 | .201 |
| △ | 10.53 | .212 |
| ○ | 10.40 | .163 |

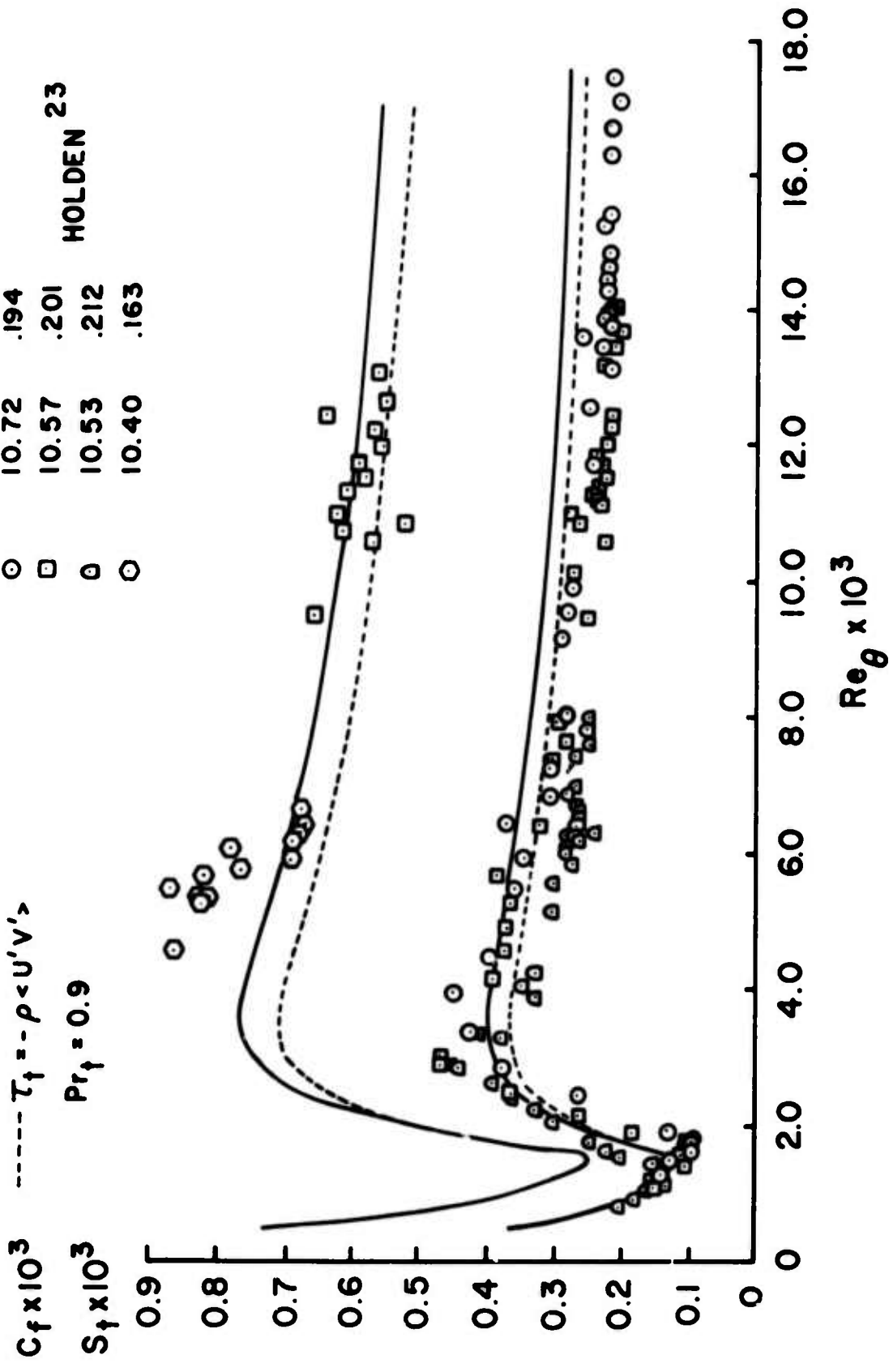


FIGURE 11 Effect of Density Fluctuation on C_f and S_f at $M_e = 10.5$

$\tau_f = -[\rho \langle u'v' \rangle + \langle \rho' u'v' \rangle]$ DATA M_e T_w/T_0
 $\tau_f = -\rho \langle u'v' \rangle$ ○ 12.04 .157 HOLDEN 23
 —+— VAN DRIEST'S THEORY 2,12

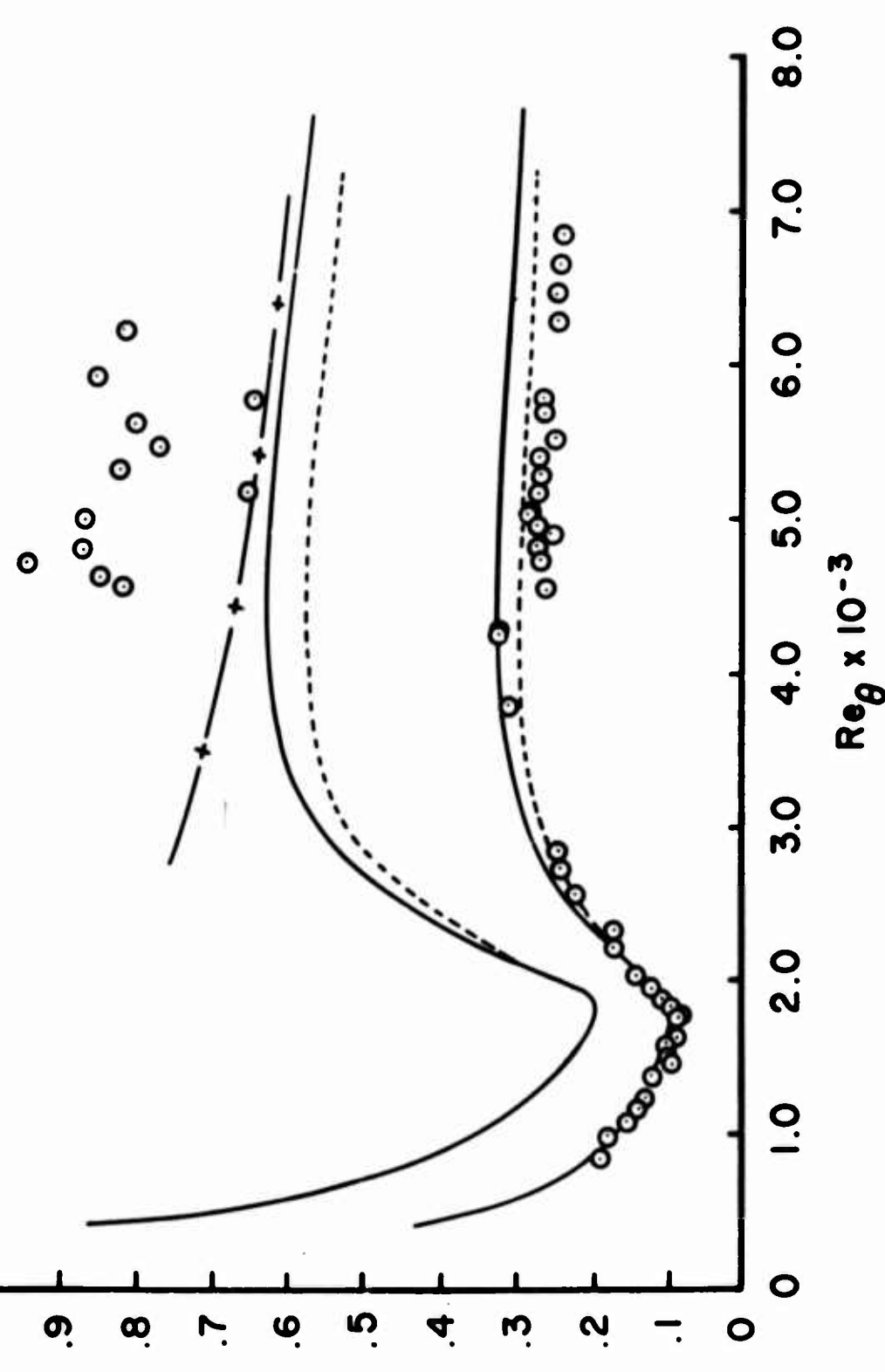


FIGURE 12 Effect of Density Fluctuation on C_f and St at $M_e = 12$

$$+ \text{---} + \tau_f = - [\rho \langle U'V' \rangle + \langle \rho'U'V' \rangle]$$

$$\text{---} \tau_f = -\rho \langle U'V' \rangle$$

C_{f_R} VAN DRIEST'S THEORY^{2,12}

DATA

- HOPKINS et al²
- HOLDEN²³

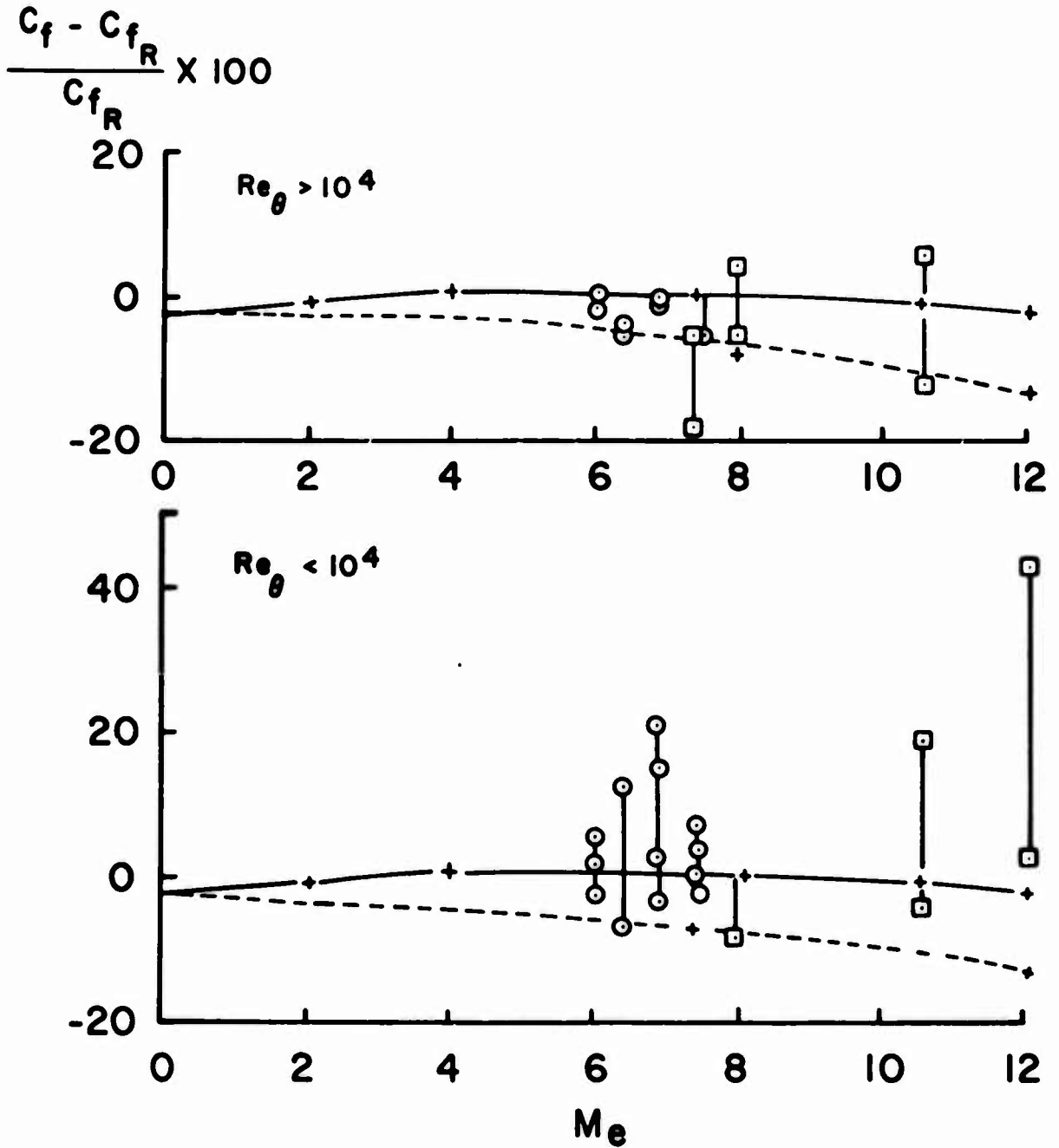


FIGURE 13 Skin Friction Coefficient Variation with Mach Number

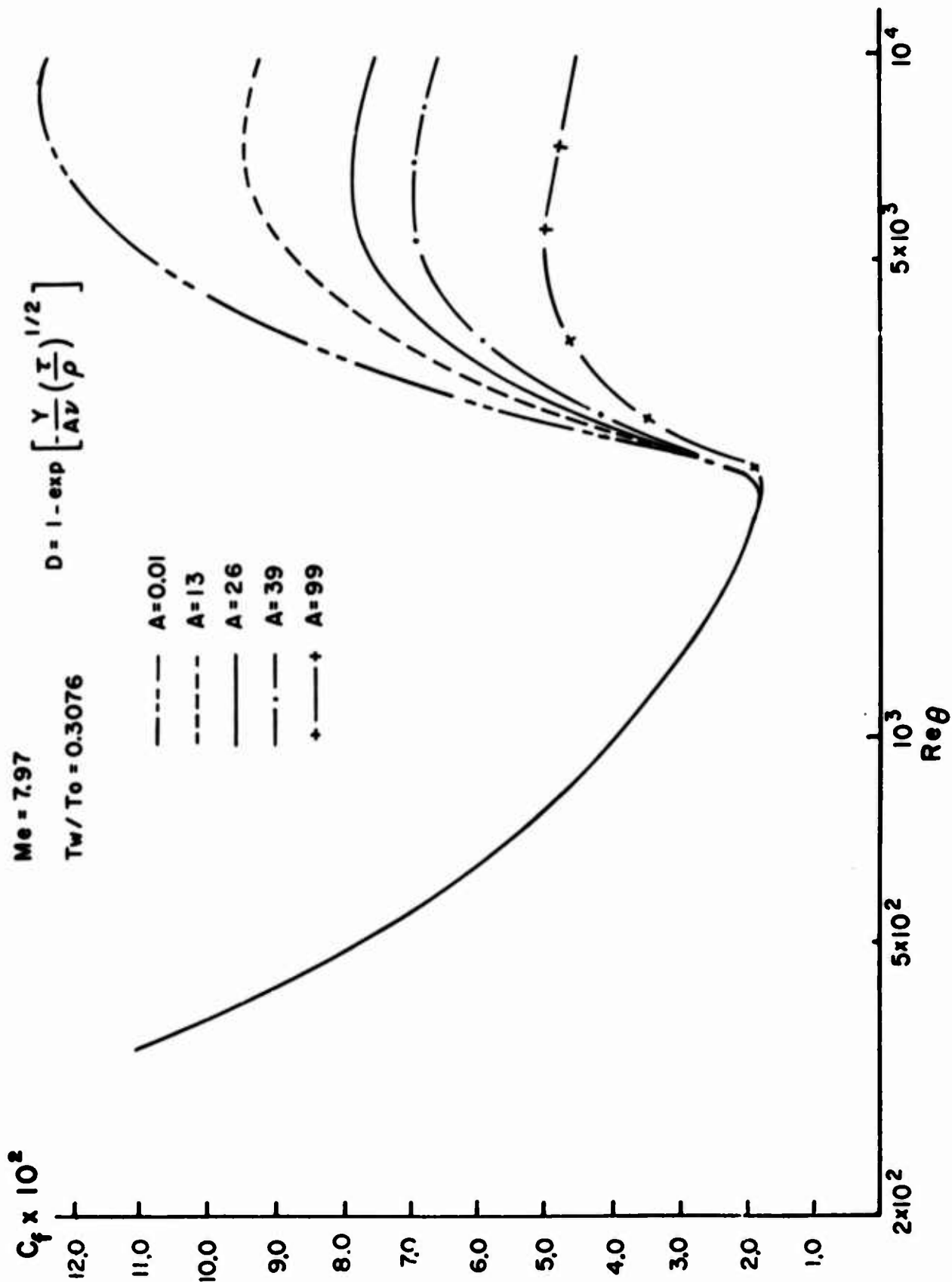


FIGURE 14 Effect of Damping Constant on C_f

REFERENCES

1. Bushnell, D. M. and Beckwith, I. E., "Calculation of Nonequilibrium Hypersonic Turbulent Boundary Layers and Comparisons with Experimental Data," AIAA Journal, Vol. 8, No. 8, August 1970, pp. 1462-1469.
2. Hopkins, E. J.; Keener, E. R.; Polek, T. E. and Dwyer, H. A., "Hypersonic Turbulent Skin Friction and Boundary-Layer Profiles on Nonadiabatic Flat Plates," AIAA Journal, Vol. 10, No. 1, January 1972, pp. 40-48.
3. Hopkins, E. J. and Keener, E. R., "Pressure Gradient Effects on Hypersonic Turbulent Skin Friction and Boundary Layer Profiles," AIAA Journal, Vol. 10, No. 9, September 1972, pp. 1141-1142.
4. Cebeci, T., "Calculation of Compressible Turbulent Boundary Layers with Heat and Mass Transfer," AIAA Journal, Vol. 9, No. 6, June 1971.
5. Shang, J. S.; Hankey, W. L. and Dwyer, D. L., "Numerical Analysis of Eddy Viscosity Models in Supersonic Turbulent Boundary Layers," AIAA Preprint 73-164, AIAA 11th Aerospace Sciences Meeting, Washington, DC, 10-12 January 1973.
6. Laderman, A. J. and Demetriades, A., "Measurements of the Mean and Turbulent Flow in a Cooled Wall Boundary Layer at Mach 9.37," AIAA Preprint 72-73, AIAA 10th Aerospace Sciences Meeting, San Diego, Calif., 17-19 January 1972.
7. Fischer, M. C.; Maddalon, D. V.; Weinstein, R. D. and Wagner, J., "Boundary Layer Pitot and Hot Wire Surveys at $M_\infty = 20$," AIAA Journal, Vol. 9, No. 5, May 1971, pp. 826-834.
8. Kistler, A. L. and Chen, W. S., "The Fluctuating Pressure Field in a Supersonic Turbulent Boundary Layer," Journal of Fluid Mechanics, 1963, pp. 41-64.
9. Meier, H. U. and Rotta, J. C., "Temperature Distributions in Supersonic

Turbulent Boundary Layers," AIAA Journal, Vol. 9, No. 11, November 1971, pp. 2149-2156.

10. Simpson, R. L.; Whitten, D. G. and Moffat, R. J., "An Experimental Study of the Turbulent Prandtl Number of Air with Injection and Suction," Int. Journal of Heat Transfer, Vol. 13, 1970, pp. 125-143.

11. Kistler, A., "Fluctuation Measurements in a Supersonic Turbulent Boundary Layer," Physics of Fluids, Vol. 2, No. 3, May-June 1959, pp. 290-296.

12. Van Driest, E. R., "Turbulent Boundary in Compressible Fluids," J.A.S., Vol. 18, No. 3, March 1951, pp. 145-160 & 216.

13. Herring, H. J. and Mellor, G. L., "A Method of Calculating Compressible Turbulent Boundary Layers," NASA CR-1144, September 1968.

14. Bradshaw, P. and Ferriss, D. H., "Calculation of Boundary-Layer Development Using the Turbulent Energy Equation: Compressible Flow on Adiabatic Walls," Journal of Fluid Mechanics, Vol. 46, Part 1, 1971, pp. 83-110.

15. Klebanoff, P. S., "Characteristics of Turbulence in a Boundary Layer with Zero Pressure Gradient," NASA TN 3178, July 1954.

16. Shang, J. S.; Hankey, W. L. and Dwyer, D. L., "Compressible Turbulent Boundary Layer Solutions Employing Eddy Viscosity Models," ARL 73-0041, February 1973.

17. Dhawan, S. and Narasimha, R., "Some Properties of Boundary Layer Flow During the Transition from Laminar to Turbulent Motion," Journal of Fluid Mechanics, Vol. 3, Part 4, 1958, pp. 418-436.

18. Kovansnay, L. S. G., "Turbulence in Supersonic Flow," J.A.S., 20, October 1953, pp. 657-675.

19. Laufer, J., "Thoughts On Compressible Turbulent Boundary Layers," Symposium on Compressible Turbulent Boundary Layers, Langley Research Center, December 1968, pp. 1.1-1.13.
20. Horstman, C. C. and Owen, F. K., "Turbulent Properties of a Compressible Boundary Layer," AIAA Journal, Vol. 10, No. 11, pp. 1418-1424.
21. Rotta, J. C., "Temperaturverteilungen in der Turbulenten Grenzschicht and der Ebenen Platte," Int. Journal of Heat Transfer, Vol. 7, 1964, pp. 215-228.
22. Laderman, A. J. and Demetriades, A., "Turbulence Measurements in the Hypersonic Boundary Layer Over a Cooled Wall," Philco-Ford Corp. Publication U-5079, September 1972, Philco-Ford Corp., Aeronutronic Div., Newport Beach, California.
23. Holden, M. S., "An Experimental Investigation of Turbulent Boundary Layers at High Mach Numbers and Reynolds Numbers," NASA CR-112147, November 1972; also Cal-AB-5072-A-1, Calspan Corporation, Buffalo, New York.
24. Huffman, G. D. and Bradshaw, P., "A Note on von Karman's Constant in Low Reynolds Number Turbulent Flows," Journal of Fluid Mechanics, Vol. 51, Part 1, 1972, pp. 45-60.